nature reviews immunology

https://doi.org/10.1038/s41577-024-00995-w

Review article

Check for updates

Mechanistic insights from inflammasome structures

Jianing Fu [1,2], Kate Schroder [3] & Hao Wu [1,2]

Abstract

Inflammasomes are supramolecular complexes that form in the cytosol in response to pathogen-associated and damage-associated stimuli, as well as other danger signals that perturb cellular homoeostasis, resulting in host defence responses in the form of cytokine release and programmed cell death (pyroptosis). Inflammasome activity is closely associated with numerous human disorders, including rare genetic syndromes of autoinflammation, cardiovascular diseases, neurodegeneration and cancer. In recent years, a range of inflammasome components and their functions have been discovered, contributing to our knowledge of the overall machinery. Here, we review the latest advances in inflammasome biology from the perspective of structural and mechanistic studies. We focus on the most well-studied components of the canonical inflammasome — NAIP–NLRC4, NLRP3, NLRP1, CARD8 and caspase-1 — as well as caspase-4, caspase-5 and caspase-11 of the noncanonical inflammasome, and the inflammasome effectors GSDMD and NINJ1. These structural studies reveal important insights into how inflammasomes are assembled and regulated, and how they elicit the release of IL-1 family cytokines and induce membrane rupture in pyroptosis.

Sections

[1]Department of Biological Chemistry and Molecular Pharmacology, Harvard Medical School, Boston, MA, USA. [2]Program in Cellular and Molecular Medicine, Boston Children's Hospital, Boston, MA, USA. [3]Institute for Molecular Bioscience, The University of Queensland, St. Lucia, Queensland, Australia. e-mail: wu@crystal.harvard.edu

Introduction

The discovery of cytosolic complexes known as inflammasomes, which promote the release of pro-inflammatory IL-1 family cytokines from cells, was a milestone event in our understanding of fever and inflammation. This key discovery built on several previous findings, including cloning of the cDNAs for IL-1α and IL-1β in 1984, and the realization that the predicted IL-1α and IL-1β proteins are larger than those that were biochemically purified from macrophage supernatant and do not have signal sequences that would account for their secretion from cells[1,2]. Soon after, the amino-terminal sequence of mature IL-1β was reported[3], confirming that a cleavage event is required for its generation. In 1992, the enzyme responsible for IL-1β cleavage was first reported as the IL-1β converting enzyme (ICE)[4,5], later renamed caspase-1 — the first member of the caspase family of cysteine proteases that mediate apoptotic and inflammatory pathways[6–8]. In 2002, the pursuit for the molecular machinery that activates caspase-1 led to the identification of the first inflammasome — the nucleotide-binding domain (NBD)-containing, leucine-rich repeat (LRR)-containing and pyrin domain-containing protein 1 (NLRP1) inflammasome — by the group of the late J. Tschopp[9]. At the time, the NLRP1 inflammasome was shown as a protein complex containing NLRP1, ASC (apoptosis-associated speck-like protein containing a caspase recruitment domain (CARD)), caspase-1 and caspase-5, but more recent data have revealed additional complexity (see below).

Rapid progress was made in the new field of inflammasomes in the subsequent years, with important clinical implications. It had previously been discovered that mutations in a relative of NLRP1 called cryopyrin (now known as NLRP3) caused a cluster of hereditary fever syndromes collectively referred to as cryopyrin-associated periodic syndromes (CAPS)[10,11]. The Tschopp group then showed that NLRP3 assembles an inflammasome with increased activity in patients with CAPS[12] or gout[13], prompting trials of the IL-1 receptor antagonist anakinra in these patients. Anakinra provided immediate and effective relief to patients with acute gout flares[14]. Patients with CAPS also responded remarkably well to anakinra[15], and IL-1-blocking agents have since remained the mainstay of the clinical management of CAPS.

These early studies defining the NLRP1 and NLRP3 inflammasomes and the first demonstration of CAPS as an inflammasome-driven human disease (an 'inflammasomopathy') paved the way for subsequent studies that characterized new inflammasome sensor molecules (for example, neuronal apoptosis inhibitory protein (NAIP)–NBD-containing, LRR-containing and CARD-containing protein 4 (NLRC4), NLRP6, absent in melanoma 2 (AIM2), pyrin and CARD8), new inflammasome effector proteases (caspase-4, caspase-5 and caspase-11), new inflammasome substrates that orchestrate cell death and alarmin release (for example, gasdermins) or sculpt tissue immune responses (for example, IL-18 and IL-37), and, most recently, the role of ninjurin 1 (NINJ1) in mediating final membrane rupture downstream of inflammasome activation (Fig. 1). In addition, a vast literature now documents hundreds of genetic and acquired inflammasomopathies, which has fuelled the development of next-generation, biologic IL-1 blockers for clinical use (rilonacept and canakinumab) and the preclinical and clinical development of small-molecule inhibitors of individual inflammasome components.

In this Review, we summarize our current understanding of the structures of inflammasome components and how these structures relate to their functions — focusing on NAIP–NLRC4, NLRP3, NLRP1, CARD8, gasdermin D (GSDMD) and NINJ1, for which recent discoveries make such review timely. These structures provide insights into how diverse protein conformational changes determine the assembly and regulation of NAIP–NLRC4 and NLRP3 inflammasomes, how autoproteolysis of NLRP1 and CARD8 enables their unique mode of activation and regulation, and how GSDMD and NINJ1 oligomerization in the membrane offers complementary mechanisms of cytokine release and membrane disruption. We do not discuss in depth several other important inflammasome sensors, including AIM2, pyrin and NLRP6. Structural studies on AIM2 are represented by earlier studies on its mode of interaction with double-stranded DNA (dsDNA)[16] and on the pyrin domain (PYD)[17–19]. Although several structures exist for certain domains in pyrin[20], and NLRP6 has been shown to form biomolecular condensates upon interaction with dsRNA and a bacterial cell wall component[21], further structural studies are required to elucidate their mechanisms of action. Furthermore, although we do not discuss these in detail, the observed differences between human and rodent inflammasomes require additional investigation. The biological aspects of inflammasome functions in health and disease have been reviewed elsewhere[22].

What makes an inflammasome?

Inflammasomes are defined as supramolecular complexes that activate inflammatory caspases; the canonical inflammasomes contain and activate caspase-1, and the noncanonical inflammasomes contain and activate caspase-4 and caspase-5 in humans and caspase-11 in mice[23–28]. Caspase-1, and now also caspase-4, have been shown to process IL-1 family cytokines (such as IL-1β and IL-18) to their mature forms[29–32]. All inflammatory caspases (caspase-1, caspase-4, caspase-5 and caspase-11) process GSDMD to induce membrane pore formation, which is responsible for releasing IL-1 family cytokines from the cell[33–35] and, together with NINJ1, for inducing a highly inflammatory form of cell death known as pyroptosis[36–45].

Inflammasomes carry out intracellular surveillance as part of the innate immune system by detecting danger signals that originate from invading microorganisms or from cellular stress or damage, defending the host and restoring cellular homoeostasis through the effects of pro-inflammatory cytokines and cell death[28,46,47] (Fig. 1). Inflammasomes have been associated with numerous human diseases, from diseases of major organs, such as the heart, liver, kidney and lung, to infection, obesity, ageing and neuroinflammation[48–53].

Canonical inflammasome components

Conceptually, the core proteins of the canonical inflammasome have three main roles: a sensor protein that is triggered by infectious or sterile danger signals resulting in its oligomerization, an adaptor protein that is recruited by the sensor upon activation, and the effector caspase-1 that executes downstream responses[27,46] (Fig. 1). Inflammasome sensors are germline encoded. However, unlike other germline-encoded innate immune receptors such as Toll-like receptors (TLRs), which directly recognize pathogen-associated molecular patterns (PAMPs) or damage-associated molecular patterns (DAMPs)[54], only some inflammasome sensors, such as NAIP, AIM2 and NLRP6, directly interact with PAMPs or DAMPs. Other inflammasome sensors, such as NLRP1 and NLRP3, detect pathogen or damage signals indirectly from their resulting cellular perturbations, which may function to discriminate between harmful and harmless stimuli without necessarily distinguishing non-self from self[27].

Most inflammasome sensors belong to the NBD-containing and LRR-containing protein (NLR) family[23,55], which comprises multi-domain proteins characterized by a central nucleotide-binding and oligomerization domain (the NACHT domain) that can bind

nucleotides (ADP or ATP) and participate in conformational changes and self-oligomerization upon activation. Twenty-two human NLRs are described, of which about nine are reported to assemble inflammasomes[55]. The NLRs are classified in subfamilies according to their amino-terminal domains: NLRPs (for example, human NLRP1, NLRP2, NLRP3, NLRP6, NLRP7, NLRP9, NLRP10 and NLRP12) have an N-terminal PYD, whereas NLRBs (also known as NAIPs, for example, human NAIP) have N-terminal baculoviral inhibitor of apoptosis repeat domains. The C-terminal domain of NLRs, with the exception of NLRP10 and NLRP1, contains an LRR domain that senses ligands or cofactors, or interacts with itself; the LRR domain for NLRP1 is in between domains, whereas NLRP10 lacks the LRR domain. Additional notable non-NLR inflammasome sensors are as follows: AIM2, which contains an N-terminal PYD and a C-terminal haematopoietic interferon-inducible nuclear (HIN) domain that binds cytosolic dsDNA[56,57]; pyrin (also known as marenostrin or TRIM20), which contains a PYD, a B-box-type zinc finger domain, a coiled-coil domain and a B30.2 (PRYSPRY) domain[58]; and CARD8, which contains a C-terminal CARD.

Upon ligand binding, resulting in activation and oligomerization, NLRP3, NLRP6, AIM2 and pyrin all recruit the adaptor protein ASC through PYD–PYD interactions[19,58–60] (Fig. 1). The structure of the ASC PYD filament was resolved in 2014 (ref. 61), and several other PYD filament structures were revealed subsequently, the latest in 2022 (refs. 17,19,62–64), confirming their similar structural architectures. For example, the PYD of AIM2, which is autoinhibited by the HIN domain based on intramolecular electrostatic interactions[18], is released by the interaction of the HIN domain with dsDNA from viral or bacterial infection[16]. It was modelled that HIN domains of multiple AIM2 molecules could wrap around dsDNA, positioning the linked PYDs on the HIN–dsDNA filament to recruit ASC[17,19]. In addition to a PYD, ASC also has a C-terminal CARD[65] that recruits caspase-1 through CARD–CARD interactions[66,67]. It is now well established that both PYD–PYD and CARD–CARD interactions generate helical assemblies to mediate homo-oligomerization and hetero-oligomerization[59,67]. Thus, ASC bridges PYD-containing upstream sensors to the downstream effector caspase-1, forming an aggregate assembly known as the 'ASC speck' or the 'inflammasome speck'[68–70].

NLRP1 has a C-terminal CARD that recruits ASC via CARD–CARD interactions, and ASC in turn recruits caspase-1. By contrast, CARD8 directly recruits and activates caspase-1 via CARD–CARD interactions without requiring the adaptor ASC[71,72]. The NAIPs, upon activation by direct binding to bacterial ligands such as flagellin, recruit the CARD-containing adaptor protein NLRC4 through NACHT–NACHT interactions in which one NAIP molecule induces conformational change and polymerization of NLRC4 to form an inflammasome disc[73–78] (Fig. 1). The CARD-containing NLRC4 can directly recruit and activate caspase-1 through CARD–CARD interactions for cell death induction, but recruitment of ASC is required for maximal pro-IL-1β processing by NAIP–NLRC4 inflammasomes[74,75,79,80].

Activation of caspase-1

Caspase-1, which is the most well-studied of the inflammatory caspases, is the effector protease of the canonical inflammasomes (Fig. 1). Caspase-1, together with the other inflammatory caspases, consists of an N-terminal CARD followed by a CARD domain linker (CDL) that connects the CARD to the protease domain. The protease domain is composed of large (~20 kDa) and small (~10 kDa) catalytic subdomains separated by an interdomain linker (IDL). Both the CDL and IDL are susceptible to proteolysis. Caspase-1 is expressed endogenously as inactive monomers. Through recruitment by the adaptor protein ASC or NLRC4, or the sensor protein CARD8, caspase-1 monomers cluster within the inflammasome platform, which induces the dimerization of their protease domains. Caspase-1 dimerization enables caspase-1 to form the full caspase catalytic domain and gain the capacity to self-cleave. Caspase-1 cleaves itself at several sites within the IDL[81] to stabilize the protease conformation and generate a dimeric species called p33/p10 (ref. 82). Caspase-1 p33/p10 is the fully active enzyme that enables the inflammasome to cleave substrates such as pro-IL-1β, pro-IL-18 and GSDMD[83]. To terminate inflammasome signalling, the active caspase-1 p33/p10 protease self-cleaves at the CDL to release the p20/p10 protease species into the cytosol, leading to dimer dissociation and shutdown of caspase-1 activity[82,83].

Noncanonical inflammasome components

The mouse noncanonical inflammasome activates caspase-11 (Fig. 1), whereas the human noncanonical inflammasomes activate caspase-4 or capase-5 (refs. 84–86). Caspase-4, caspase-5 and caspase-11 are inflammatory caspases with a similar domain structure to caspase-1 and, like caspase-1, they are expressed in resting cells as inactive monomers that require dimerization to acquire protease activity[29,87]. However, unlike the caspase-1-containing canonical inflammasomes, the noncanonical inflammasomes are lipid–protein assemblies in which the CARDs of caspase-4, caspase-5 and caspase-11 interact directly with bacterial lipopolysaccharide (LPS) or endogenous oxidized phospholipids to facilitate the activation of their latent protease function[84–86]. Although the stoichiometry of ligand to caspase within this assembly is unclear, it is expected that noncanonical inflammasome complexes induce the formation of caspase dimers and, perhaps, higher-order oligomers. Dimerization of caspase-4, caspase-5 and caspase-11 confers the capacity to self-cleave at the IDL to generate p32/p10 dimers with maximal protease activity[29,87,88]. Whereas caspase-11 cannot cleave pro-IL-1β, recent studies suggest that self-cleavage of caspase-4 at IDL residue D289 generates a p34/p9 protease species that directly cleaves pro-IL-1β, albeit weakly[29]. Caspase-4 can also process pro-IL-18, as shown by multiple studies[30–32]. The recent cryo-electron microscopy (cryo-EM) and crystal structures of caspase-4 in complex with pro-IL-18 have revealed a two-prong interaction mode in which the binding site outside of the active site (known as the exosite) strengthens and orients the binding site at the active site to enable proteolytic processing[89,90]. Caspase-4, caspase-5 and caspase-11 cleave GSDMD to generate transmembrane pores to initiate pyroptosis[37–42,91] or pyroptosis-associated expulsion of neutrophil extracellular traps[92,93]; in so doing, these caspases induce a second wave of inflammasome signalling via NLRP3 activation by GSDMD-mediated membrane damage and K^+ efflux.

NAIP–NLRC4 inflammasomes

NAIPs are cytosolic receptors for various bacterial protein ligands, resulting in recruitment of the adaptor protein NLRC4 to form NAIP–NLRC4 inflammasomes[74,75,94–97] (Fig. 2a). There are seven NAIP paralogues in mice (NAIP1 to NAIP7) but only one NAIP in humans. Different mouse NAIPs are specific for different bacterial ligands, among which NAIP5 and NAIP6 recognize bacterial flagellin, the major protein in the bacterial flagellum, and NAIP1 and NAIP2 recognize needle and inner rod proteins, respectively, of the type III secretion system. Although human cells have only one NAIP, they have been shown to respond to both flagellin and needle protein of the type III secretion system, perhaps depending on different splicing isoforms[95,98].

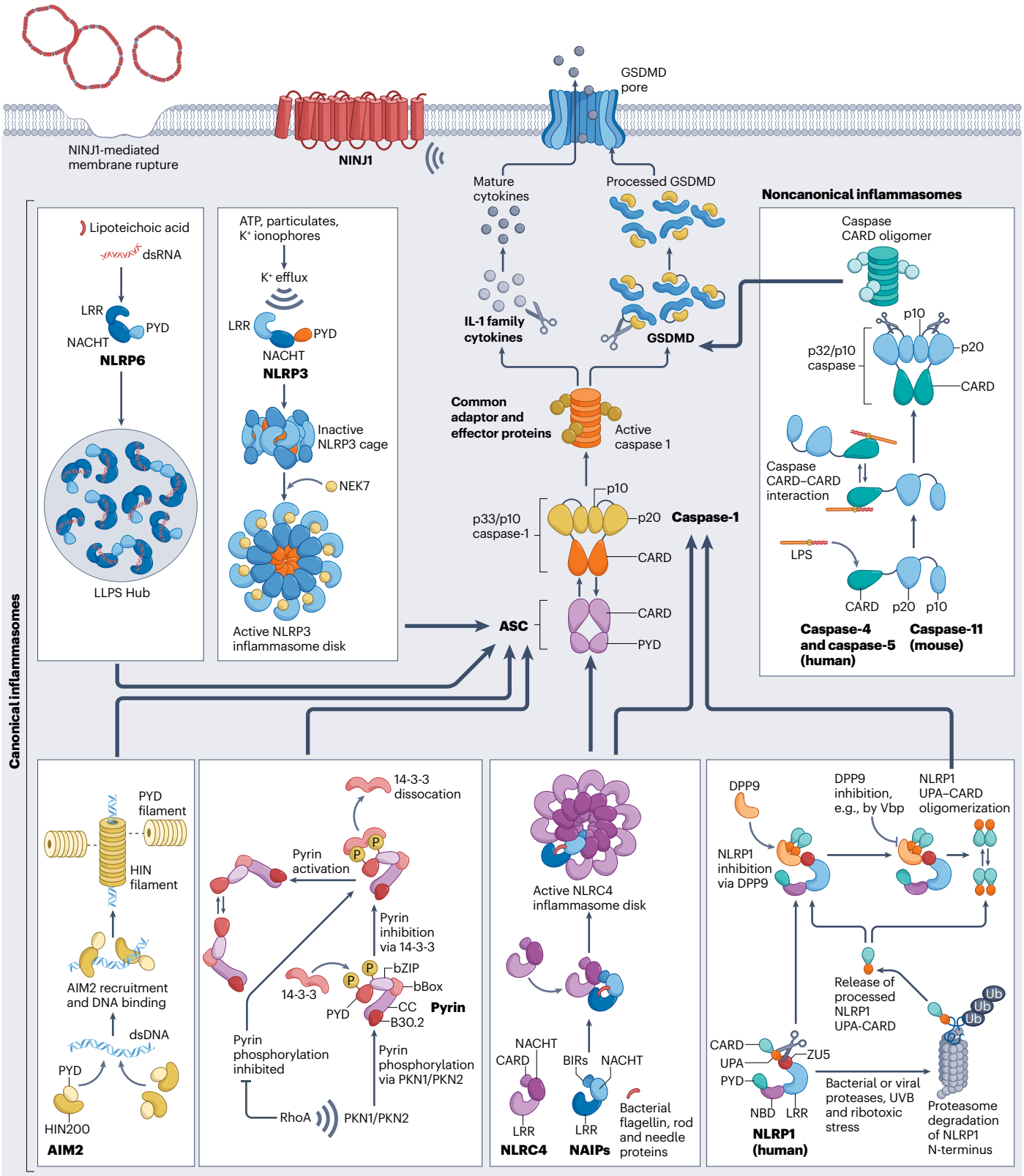
NINJ1-mediated membrane rupture
NINJ1
GSDMD pore
Mature cytokines
Processed GSDMD
IL-1 family cytokines
GSDMD
Common adaptor and effector proteins
Active caspase 1
p10
p33/p10 caspase-1
p20
Caspase-1
CARD
ASC
CARD
PYD
Canonical inflammasomes
Lipoteichoic acid
dsRNA
LRR
PYD
NACHT
NLRP6
LLPS Hub
ATP, particulates, K+ ionophores
K+ efflux
LRR
PYD
NACHT
NLRP3
Inactive NLRP3 cage
NEK7
Active NLRP3 inflammasome disk
Noncanonical inflammasomes
Caspase CARD oligomer
p10
p32/p10 caspase
p20
CARD
Caspase CARD–CARD interaction
LPS
CARD
p20
p10
Caspase-4 and caspase-5 (human)
Caspase-11 (mouse)
PYD filament
HIN filament
AIM2 recruitment and DNA binding
dsDNA
PYD
HIN200
AIM2
14-3-3 dissociation
Pyrin activation
Pyrin inhibition via 14-3-3
bZIP
bBox
14-3-3
PYD
CC
B30.2
Pyrin
Pyrin phosphorylation inhibited
Pyrin phosphorylation via PKN1/PKN2
RhoA
PKN1/PKN2
Active NLRC4 inflammasome disk
NACHT
CARD
LRR
NLRC4
BIRs
NACHT
LRR
NAIPs
Bacterial flagellin, rod and needle proteins
DPP9
NLRP1 inhibition via DPP9
DPP9 inhibition, e.g., by Vbp
NLRP1 UPA–CARD oligomerization
Release of processed NLRP1 UPA-CARD
Ub
CARD
UPA
PYD
ZU5
NBD
LRR
NLRP1 (human)
Bacterial or viral proteases, UVB and ribotoxic stress
Proteasome degradation of NLRP1 N-terminus
Homotypic interaction
Stage of the inflammasome pathway
Binding, attachment or dissociation
Indirect activation signal

Fig. 1 | The canonical and noncanonical inflammasome pathways. The figure summarizes the canonical inflammasomes comprising NLRP1, NLRP3, NLRP6, NAIP–NLRC4, AIM2 and pyrin, the noncanonical inflammasomes formed by caspase-4 and caspase-5 (human) and caspase-11 (mouse), and the adaptor and effector proteins associated with these pathways, notably the adaptor ASC and the effectors caspase-1, IL-1 family cytokines, GSDMD and NINJ1. Shown are the major protein domains involved in structural organization and function. For more detailed descriptions of each pathway, see the main text. AIM2, absent in melanoma 2; ASC, apoptosis-associated speck-like protein containing a CARD; BIR, baculoviral inhibitor of apoptosis repeat; CARD, caspase recruitment domain; DPP, dipeptidyl peptidase; dsDNA, double-stranded DNA; GSDMD, gasdermin D; HIN, haematopoietic interferon-inducible nuclear; LLPS, liquid–liquid phase separation; LPS, lipopolysaccharide; LRR, leucine-rich repeat; NACHT, nucleotide-binding and oligomerization domain; NAIP, neuronal apoptosis inhibitory protein; NBD, nucleotide-binding domain; NINJ1, ninjurin 1; NLRC, NAIP–NBD-containing, LRR-containing and CARD-containing protein; NLRP, NBD-containing, LRR-containing and PYD-containing protein; PYD, pyrin domain; UVB, ultraviolet B radiation; VbP, Val-boro-pro (DPP8 and DPP9 inhibitor).

The mechanism by which NAIP–NLRC4 inflammasomes are assembled and activated has been elucidated from a series of structural and biochemical studies. When the crystal structure of NLRC4 was first solved, it showed an autoinhibited, closed conformation[76] (Fig. 2b). Subsequently, reconstitution of the complex of NAIP2 and NLRC4 with the rod protein PrgJ of *Salmonella enterica* subsp. *enterica* serovar Typhimurium suggested that each disc-shaped inflammasome contains one copy of NAIP2 and PrgJ but multiple copies of NLRC4; cryo-EM structures of 10-fold, 11-fold or 12-fold averaged discs contained mostly NLRC4 (refs. 73,77). The active conformation of NLRC4 in these structures revealed a rotation of close to 90° within the NACHT domain, between its first two subdomains (NBD and helical domain 1 (HD1)) and its last two subdomains (winged helix domain (WHD) and helical domain 2 (HD2)), together with the LRR domain, to open up the structure. This conformational change in NLRC4 seemed to be initiated by binding to PrgJ-bound NAIP2, and it was successively propagated to other NLRC4 molecules in the disc by nucleated polymerization (Fig. 2b).

The conformation of ligand-bound NAIP5 was revealed by cryo-EM structures of a flagellin-bound NAIP5 in complex with an NLRC4 mutant that does not self-associate[99], and of the wild-type flagellin–NAIP5–NLRC4 disc solved without applying symmetry[100]. Flagellin was shown to bind in a deep pocket formed by multiple domains of NAIP5, a strategy that was suggested to limit the potential for immune evasion by the pathogen[100]. Ligand binding seemed to open up NAIP5 into an active conformation similar to the active NLRC4 structure. However, a recent cryo-EM structure of ligand-free NAIP5 revealed an unprecedented open structure that was accessible to recruit inactive NLRC4 (ref. 78) (Fig. 2b). Ligand binding to NAIP5 induces a small rotation in the WHD of the NACHT domain that creates a steric clash with inactive NLRC4 and places a loop for optimal interaction with active NLRC4, thus both triggering and stabilizing the conversion of NLRC4 to the active state (Fig. 2b).

The NLRP3 inflammasome

NLRP3 is expressed in immune cells such as macrophages, dendritic cells and neutrophils[101], but at a low level under resting conditions that is not sufficient to initiate NLRP3 inflammasome formation. Thus, a 'priming' step is needed to first upregulate the expression of NLRP3 in most cell types[28,102–104]; the need for priming is shared by some inflammasomes such as NLRP6 (ref. 105) but is not required for others such as the NAIP–NLRC4 or AIM2 inflammasomes. The reason for this additional step is not clear but it is suggested that priming might help to better regulate inflammasome activation, particularly given that both NLRP3 and NLRP6 can be activated by many stimuli. The pro-IL-1β protein also often requires priming as it is usually not expressed without stimulation[106], in contrast to pro-IL-18, which is constitutively expressed in various cell types[106] but can be further upregulated under specific conditions[107]. Acute LPS treatment has been shown to prime NLRP3 activation even in the presence of the protein synthesis inhibitor cycloheximide, which suggests that priming can occur in a non-transcriptional manner, probably involving posttranslational modifications such as deubiquitylation and phosphorylation[104,108–113].

After priming, NLRP3 can be activated by microbial infection and by sterile insults that trigger certain cellular perturbations[28,46]. Potassium (K^+) efflux is a pivotal upstream event for NLRP3 inflammasome activation, with high extracellular K^+ concentration having an inhibitory effect[114–116]. Widely used NLRP3 activators support the role of K^+ efflux in inflammasome activation: nigericin is a bacterial toxin and K^+ ionophore[117], extracellular ATP gates the P2X7 cation channel for Ca^{2+} and Na^+ influx and in turn activates the potassium channel TWIK2 (also known as KCNK6) for K^+ efflux[117,118], and particulate matter induces a decrease of intracellular K^+ concentration and increase of intracellular Ca^{2+} concentration[116]. Of note, spontaneous K^+ efflux in response to low extracellular K^+ concentration also activates NLRP3 (ref. 116). Nonetheless, because ionic fluxes in cells are often coupled, whether K^+ concentration, or that of another ion, is the key inducer of the NLRP3 inflammasome remains controversial. In particular, whereas some studies have suggested that K^+ efflux regulates Ca^{2+} signalling to activate the NLRP3 inflammasome[119], other studies have suggested that K^+ efflux induces NLRP3 inflammasome activation independently of Ca^{2+} signalling[120].

Crystals and particles that activate NLRP3 include monosodium urate crystals[13], aluminium hydroxide, silica, asbestos[121,122], cholesterol crystals[123,124] and amyloid-β (ref. 125), which are associated with gouty arthritis, pulmonary and cardiovascular diseases, and Alzheimer disease. Malarial hemozoin is also an NLRP3 inflammasome activator owing to its particulate nature, and inflammasome activation may contribute to the recurrent fever attacks and neurodegeneration that are associated with malaria[126]. Activation of NLRP3 by particulate matter seems to involve their phagocytosis and subsequent lysosomal damage and rupture[121,125]. The importance of lysosomal damage in inflammasome activation is supported by the ability of the lysosomal damage inducer, leucyl-leucine methyl ester, to activate NLRP3 (ref. 121). However, how lysosomal damage is associated with K^+ efflux remains unknown[116,119,121]. Other factors such as reactive oxygen species, mitochondria and oxidized mitochondrial DNA have also been implicated in NLRP3 activation[127–130]. In addition, several agents that activate NLRP3 independently of K^+ efflux have been described, including the TLR agonists imiquimod and CL097, which activate NLRP3 independently of TLR signalling[131].

The NLRP3 inflammasome has been heavily investigated owing to its biological significance and therapeutic relevance, which have recently been reviewed elsewhere[22,55]. Here, we focus on describing the structural nature of NLRP3 — from its interaction with NEK7 to the inactive oligomer structure that we refer to as a 'cage' and to the active

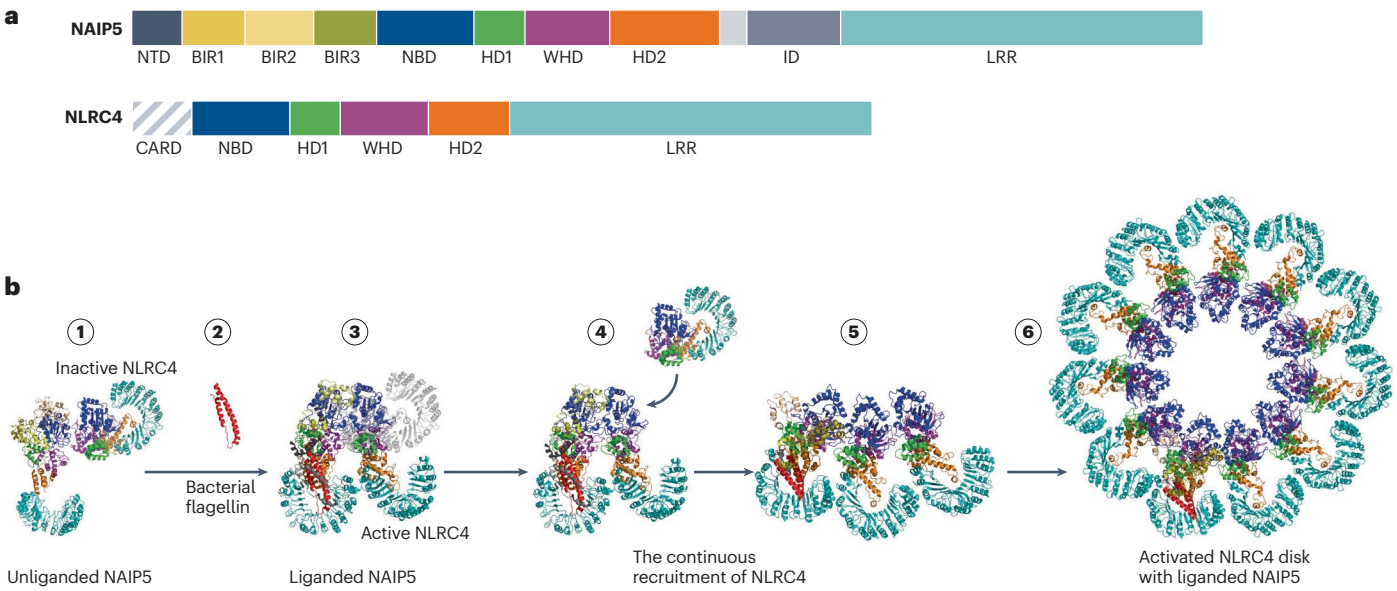

Fig. 2 | The NAIP–NLRC4 inflammasome. NAIP5, a typical NAIP, and flagellin, a NAIP5 ligand, are used as examples. **a**, Domain architectures of NAIP5 and NLRC4, with the domain colours matching those shown in part **b**. Domains that are shown in grey indicate that the structure of this specific region is not shown in part **b**. **b**, Formation of the NAIP5–NLRC4 inflammasome. Step 1: the unliganded NAIP5 (Protein Data Bank [PDB:7RAV]) and inactive NLRC4 [PDB:4KXF] at resting state, shown as a weak dimer complex. NAIP5 and NLRC4 can also be monomers before activation. Step 2 and step 3: the interaction between bacterial flagellin and NAIP5 induces the activation of NAIP5 [PDB:5YUD] and NLRC4 [PDB:4KXF], together with conformational changes. The grey NLCR4 molecule in step 3 represents the inactive state before its conformational changes to the active state. Step 4 to step 6: the activated NLRC4 self-propagates [PDB:6B5B], building up an inflammasome disc [PDB:3JBL]. Domains are colour coded as in part **a**. NAIP2 follows the same mechanism in forming an inflammasome disc. BIR, baculoviral inhibitor of apoptosis repeat; CARD, caspase recruitment domain; HD, helical domain; ID, intermediate domain; LRR, leucine-rich repeats; NAIP, neuronal apoptosis inhibitory protein; NBD, nucleotide-binding domain; NLRC, NAIP–NBD-containing, LRR-containing and CARD-containing protein; NTD, N-terminal domain; WHD, winged helix domain.

disc-like structure with ASC — which collectively begin to sketch out a series of conformational changes that occur in the NLRP3 activation pathway.

Structure of the NLRP3(ΔPYD)–NEK7 complex

The first NLRP3 structure was determined in 2019 (ref. 132) following the discovery of NEK7 as an essential factor in mouse NLRP3 activation[133–135]. NEK7 is a centrosomal serine/threonine kinase; for NLRP3 activation, the kinase scaffold but not the kinase activity is required. A PYD-deleted (ΔPYD) human NLRP3 construct was shown to form a complex with human NEK7 at a sub-micromolar binding affinity[132]. The stability of NLRP3 and of the NLRP3–NEK7 complex was increased by the addition of ADP and the specific NLRP3 inhibitor MCC950 to the samples for cryo-EM structure determination[136]. This ability to reconstitute a complex between inactive NLRP3 and NEK7 suggested that NEK7 is not the direct activator of NLRP3, despite its requirement to form an active NLRP3 inflammasome. Of note, although the role of NEK7 has been demonstrated in mouse cells and in mice, its function in human cells has been controversial. In particular, a recent study has suggested that in human cell lines, NEK7 is redundant for inflammasome activation when the nuclear factor-κB regulator IKKβ is activated during priming but it can synergize with IKKβ to shorten the priming requirement for NLRP3 activation[137].

The NLRP3(ΔPYD)–NEK7 structure revealed a first glimpse of inactive NLRP3, from its central NACHT domain to the C-terminal LRR domain[132] (Fig. 3a). Whereas ADP was shown to bind the NACHT domain, the location of MCC950 binding was not determined owing to the limit in resolution. The NLRP3 NBD and HD2 (subdomains of NACHT) and the LRR domain contact the C-terminal lobe of NEK7 and assume a tight grip around it; the N-terminal lobe of NEK7 is disordered in this structure. Structure-based mutagenesis of the binding interface indicated that the LRR domain and HD2 of NLRP3 are important for NEK7 binding whereas the NBD is dispensable. This conclusion is consistent with the hypothesis that NEK7 most probably is recruited after NLRP3 has changed to its active conformation, when the NBD is rotated out of the vicinity of NEK7 (ref. 138). Thus, the NLRP3–NEK7 structure provides the molecular basis for NEK7 recruitment to the NLRP3 oligomer.

Structure of NLRP3 'cages'

Structures of full-length NLRP3 as determined by cryo-EM were shown to exist as double-ring-shaped cages, with human NLRP3 forming decamers and mouse NLRP3 forming dodecamers to hexadecamers[139–141] (Fig. 3b). These NLRP3 oligomers are referred to as cages because the PYDs of the NLRP3 molecules, which are important for ASC recruitment and inflammasome assembly, seem to be shielded within the cages, possibly to prevent premature activation[140]. In all structures, the cages are formed by interactions between the LRR domains of the two NLRP3 rings, together with interactions between the PYDs[139–141]. Although the PYD–PYD interactions were not directly visualized as ordered densities, low-resolution densities were observed and the PYDs are important for cage formation. These data were interpreted

as the existence of PYD filaments within the cage in one study[140] but were modelled as two PYD molecules in another study[139].

Surprisingly, NLRP3 cages are mainly membrane bound, as shown by fractionation experiments in NLRP3-overexpressing cells or macrophage cell lines endogenously expressing NLRP3, despite NLRP3 not being a bona fide transmembrane protein[140]. This observation is consistent with earlier studies showing the localization of NLRP3 at various intracellular organelles before NLRP3 activation[142]. Immunofluorescence imaging of wild-type, immortalized bone marrow-derived macrophages revealed partial localization of NLRP3 at the trans-Golgi

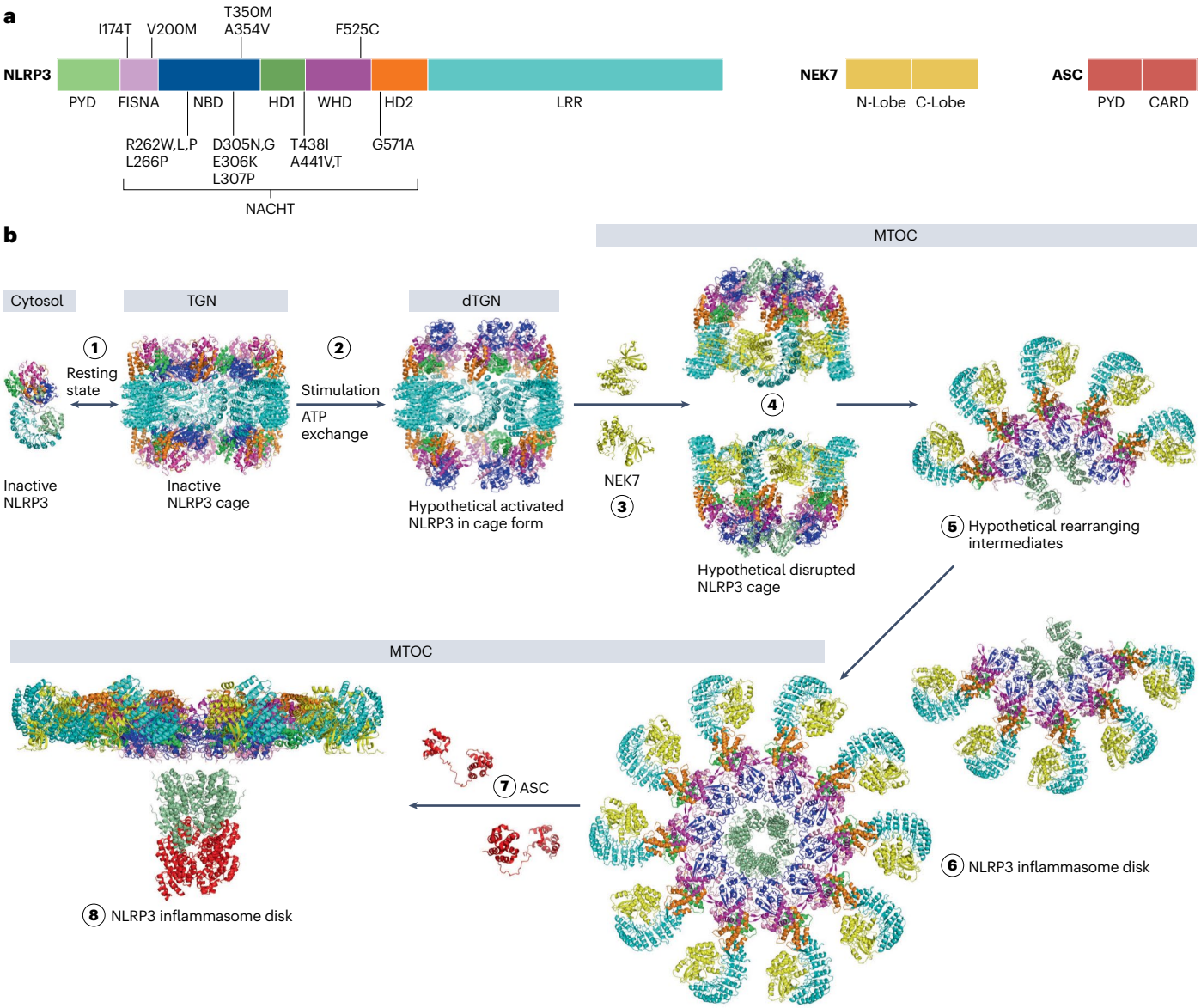

Fig. 3 | The NLRP3 inflammasome. a, Domain architectures of NLRP3, NEK7 and ASC, with the domain colours matching those shown in part **b**. Typical disease-associated mutations in NLRP3 are highlighted. **b**, Formation of the NLRP3 inflammasome. Step 1: upon upregulation of their expression ('priming'), NLRP3 proteins are present in the cytosol and on the trans-Golgi network (TGN) as monomeric proteins or inactive 'cage' structures [PDB:7PZC]. Step 2: upon stimulation, inactive NLRP3 cages presumably undergo conformational changes. The TGN disperses into vesicles (dispersed TGN (dTGN)) containing hypothetical active NLRP3 cages. Step 3: via microtubule trafficking, the vesicles move to the microtubule organizing centre (MTOC), wherein NEK7 [PDB:6S76] proteins are located. Step 4 and step 5: NEK7 interacts with NLRP3 cages [PDB:6NPY], presumably disrupting and opening each cage into two halves. Step 6: the two halves rearrange and unite into an inflammasome disc [PDB:8EJ4 and PDB:8ERT]. Step 7 and step 8: ASC [PDB:2KN6] adaptor proteins are recruited to the NLRP3 inflammasome disc via homotopic PYD–PYD interactions [PDB:8EJ4, PDB:8ERT and PDB:3J63], resulting in a PYD–PYD filament that oligomerizes the CARDs of ASC molecules to mediate caspase-1 recruitment. Domains are colour coded as in part **a**. ASC, apoptosis-associated speck-like protein containing a CARD; CARD, caspase recruitment domain; FISNA, fish-specific NACHT-associated domain; HD, helical domain; LRR, leucine-rich repeats; NACHT, nucleotide-binding and oligomerization domain; NBD, nucleotide-binding domain; NLRP, NBD-containing, LRR-containing and PYD-containing protein; PYD, pyrin domain; WHD, winged helix domain.

network (TGN), as marked by TGN38, and this localization was further increased when NLRP3 was stably expressed to reconstitute NLRP3-knockout cells[140]. Interestingly, the TGN disperses into vesicles marked by TGN38 known as dispersed TGN (dTGN) in response to NLRP3 stimuli[143], and NLRP3 mutants that cannot form cages are defective in both TGN dispersion and NLRP3 activation[140].

Another study has suggested that NLRP3 inflammasome activators converge on disrupting endoplasmic reticulum–endosome membrane contact sites, causing endosomal accumulation of phosphatidylinositol 4-phosphate (PI4P) and a consequent impairment of endosome-to-TGN trafficking[144]. In this context, endosomes can accumulate TGN38, giving them the appearance of dTGN vesicles. The TGN dispersion model of NLRP3 may, thus, be unifiable with the endosomal model in that both models involve the accumulation of PI4P-enriched vesicles that recruit NLRP3. Of note, in studies involving changes to extracellular K^+ concentration, it was suggested that K^+ efflux is essential for NLRP3 recruitment to vesicles and NLRP3 activation. By contrast, when NLRP3 recruitment to vesicles was forced by fusing the protein to a Golgi-localization domain, then increased extracellular K^+ concentration had no effect on NLRP3 activation[143].

Structure of the active NLRP3 inflammasome

The first indication that NLRP3 is associated with the microtubule-organizing centre (MTOC) came from the identification of the centrosomal kinase NEK7 as an essential factor in NLRP3 activation[133–135]. Indeed, the NLRP3 inflammasome has been shown to localize at the MTOC to form the caspase-1 p33/p10 active enzyme[145,146], and microtubule retrograde transport by dynein and a dynein adaptor, HDAC6, is required for this MTOC localization of NLRP3 and for inflammasome activation. As the TGN marker TGN38 was detected at the MTOC upon inflammasome activation, and NEK7 can decrease the amount of NLRP3 cages in vitro, it was proposed that NLRP3 cages are transported on vesicles to the MTOC wherein they bind NEK7 and change their structural organization[140,146].

The cryo-EM structure of an active NLRP3 inflammasome was solved recently after optimizing the reconstitution method[138] (Fig. 3b). NLRP3 and NEK7 were co-transfected and expressed in human Expi293 cells and stimulated with the NLRP3 activator nigericin before harvesting. Previous studies using an engineered NLRP3 with a bioluminescence resonance energy transfer (BRET) sensor have suggested that nigericin or other K^+ ionophores alter NLRP3 conformation in a K^+ efflux-dependent manner[147], a process that has not been achievable using recombinant proteins probably owing to the requirement of membranes. The BRET study has also revealed the importance of the fish-specific NACHT-associated (FISNA) domain of NLRP3 (ref. 147) — an additional NACHT subdomain, in front of the NBD — in mediating this conformational change, which was confirmed by the active NLRP3 inflammasome structure[138]. The successful reconstitution of the active NLRP3 inflammasome required the addition of Mg^{2+} and ATPγS, presumably to keep NLRP3 in an active conformation, and of ASC PYD, to further promote NLRP3 inflammasome formation. The requirement for ASC to assemble a stable NLRP3 inflammasome is in contrast to the previously solved NAIP–NLRC4 inflammasome structure (without ASC)[73].

The active NLRP3–NEK7–ASC complex comprises mainly 10 or 11 individual subunits of NLRP3, with the 10-fold structure being more prevalent and solved at a higher resolution[138] (Fig. 3b). The NLRP3–NEK7 complex forms a disc-shaped structure with the NACHT domains of NLRP3 near the disc centre and the NEK7-bound LRR domains of NLRP3 at the periphery. The PYDs of NLRP3 form a PYD filament that protrudes orthogonally from the centre of the disc, which further recruits ASC through PYD–PYD interaction. The hybrid NLRP3–ASC PYD filament structure is similar to the PYD filament structures of ASC and NLRP3 separately[59,62]. There is a symmetry mismatch between the disc and the filament, probably made possible by the flexible linker between the PYD and the NACHT domain of NLRP3. Large-scale conformational changes are observed between the ADP-bound inactive NLRP3 conformation[132] and the ATP-bound active NLRP3 conformation[138], which are reflected by a rotation of approximately 85° between the FISNA–NBD–HD1 region of NLRP3 and the WHD–HD2–LRR region, and by local conformational changes in particular at the FISNA domain. Interactions at the centre of the disc are dominated by the FISNA domain, with additional contributions from NBD, HD1 and WHD[138].

Intriguingly, each NEK7 molecule binds to only one NLRP3 molecule and does not participate in NLRP3 oligomerization in the disc[138]. Thus, we propose that the function of NEK7 is to break inactive NLRP3 cages to allow for reassembly. Although this disc structure provides a framework for understanding NLRP3 biology, many additional proteins can modulate NLRP3 inflammasome assembly, such as BTK[148], MAVS[149,150] and NLRP11 (ref. 151), and numerous posttranslational modifications of NLRP3 have been identified[25,152–154], which open up the possibility that NLRP3 cross-talks with a large number of cellular pathways to regulate its activation. Interestingly, the minimal requirement for NEK7 for NLRP3 inflammasome activation in human cell lines was shown to be attributable to IKKβ-induced recruitment of NLRP3 to the TGN during priming[137]. Whether NEK7-independent inflammasome activation alters microtubule-mediated trafficking and the localization of NLRP3 inflammasome specks remains to be addressed.

NLRP1 and CARD8 inflammasomes

Although NLRP1 was the first protein to be identified as forming a caspase-1-activating complex[9], its activation mechanism was not elucidated until much later. Like other NLRPs, human NLRP1 contains a PYD at the N-terminus. However, the PYD of NLRP1 has an autoinhibitory function rather than recruiting ASC to form the inflammasome. In support of this, mutations in NLRP1 PYD cause hyperactivation and have been associated with inflammatory skin diseases[155,156]. In addition to a PYD, and NACHT and LRR domains, NLRP1 also contains a unique function-to-find domain (FIIND) followed by a CARD at the C-terminus[157] (Fig. 4a). The FIIND, composed of ZU5 and UPA subdomains, undergoes autoproteolytic cleavage at a Ser–Phe–Ser motif at the C-terminal end of ZU5, generating an N-terminal PYD–NACHT–LRR–ZU5 fragment that is autoinhibitory and a C-terminal UPA–CARD fragment that activates the inflammasome[158]. This autocleavage event is required for NLRP1 function, and it is important that the N-terminal and C-terminal fragments remain associated with each other at the resting state[159–162].

It is now established that proteasome-dependent 'functional degradation' of the N-terminal fragment is the main mechanism by which NLRP1 is activated[159,161,163]. It has been observed that anthrax lethal factor cleaves the N-terminal domain of NLRP1b, a mouse NLRP1 orthologue naturally lacking a PYD, resulting in inflammasome activation[164–166]. Upon cleavage, the N-terminal fragment undergoes ubiquitylation by the N-end rule ligase UBR2 (refs. 159,167), leading to its proteasomal degradation and liberation of the C-terminal fragment for inflammasome activation[159,161] (Fig. 4a). *Shigella flexneri* ligase IpaH7.8 directly ubiquitylates NLRP1b, also resulting in proteasomal degradation and inflammasome activation[161,163]. Moreover, the prolyl dipeptidyl peptidases DPP8 and DPP9 have been shown to associate with and

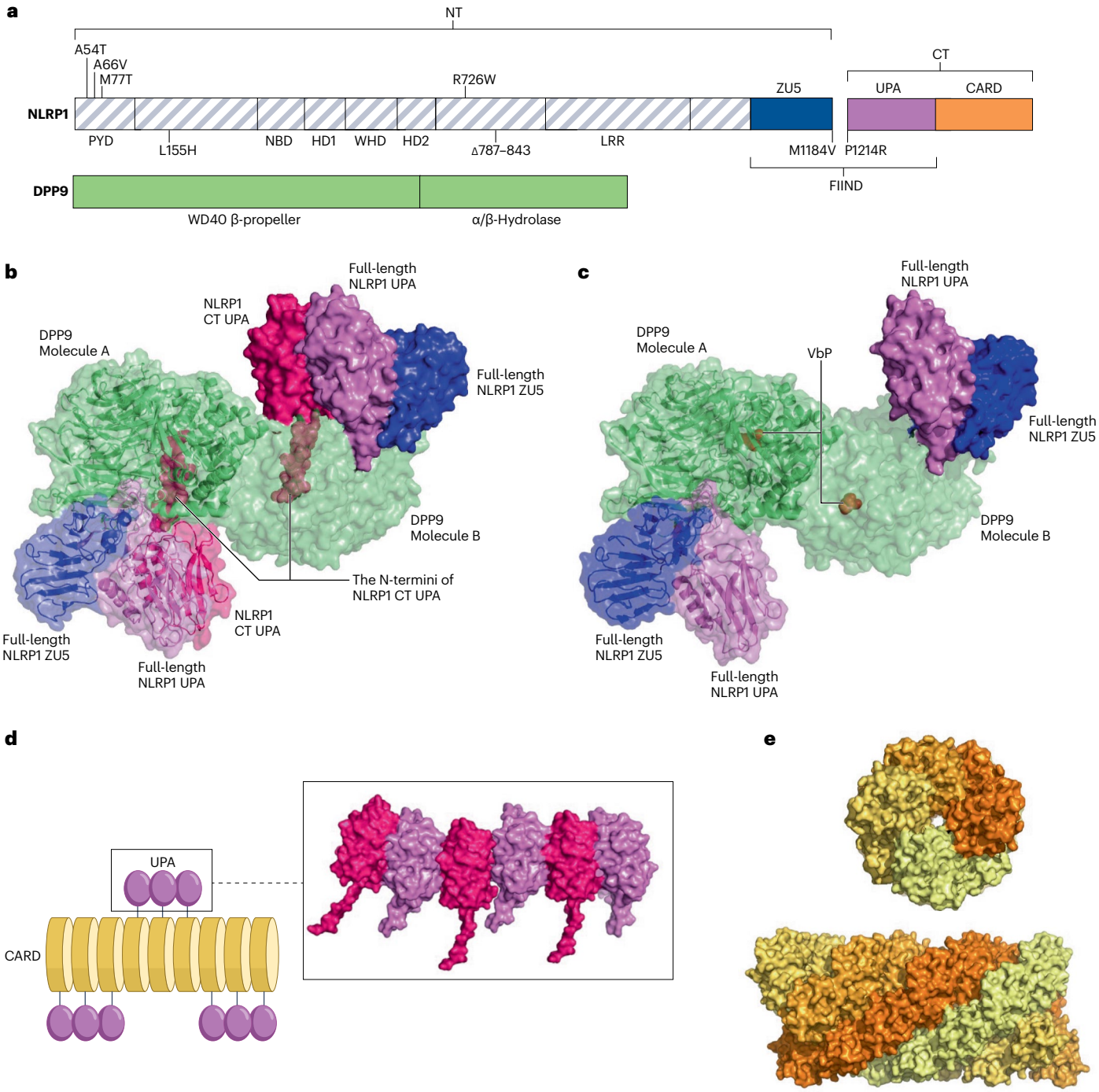

Fig. 4 | The NLRP1 inflammasome. a, Domain architectures of NLRP1 and DPP9. Domains that are shown in grey indicate that the structure of this specific region is not shown in parts **b**–**e**. The unlabelled domains in NLRP1 represent predicted unstructured regions. Typical disease-associated mutations in NLRP1 are highlighted. The proteolysis site on the FIIND is marked as a gap. **b**, The structure of an NLRP1 and DPP9 ternary complex, a dimeric complex in which each half of the dimer contains ZU5 and UPA (the FIIND) of full-length NLRP1, the UPA of a processed NLRP1 C-terminal fragment and a DPP9 monomer [PDB:6X6A]. The N-terminal end of the NLRP1 C-terminal UPA inserts into the active-site tunnel of DPP9. **c**, The structure of DPP9 bound with the small-molecule inhibitor Val-boro-pro (VbP) in complex with NLRP1 [PDB:6X6C]. VbP occupies the active site of DPP9, which releases the NLRP1 C-terminal UPA, allowing for the activation of NLRP1. **d**, Clustering of NLRP1 UPA [PDB:6XKK] promotes the homotypic interactions of NLRP1 CARDs to form filaments. **e**. Two different orientations of an NLRP1 CARD filament [PDB:6K7V]. For parts **b**–**e**, domains are colour coded as in part **a**. CARD, caspase recruitment domain; CT, C-terminus; DPP, dipeptidyl peptidase; FIIND, function-to-find domain; HD, helical domain; LRR, leucine-rich repeats; NBD, nucleotide-binding domain; NLRP, NBD-containing, LRR-containing and PYD-containing protein; NT, N-terminus; PYD, pyrin domain; WHD, winged helix domain.

inhibit NLRP1 inflammasome activation, and small-molecule inhibitors of DPP8 and DPP9, such as Val-boro-pro (VbP), activate the NLRP1 inflammasome by a proteasome-dependent mechanism[159,168–171].

Ultraviolet B (UVB) radiation is another stimulus that is known to induce NLRP1 activation in human, but not rodent, keratinocytes[172,173], and ribosome stalling caused by UVB radiation to mediate the ribotoxic stress response has been associated with activation of the mitogen-activated protein kinase ZAKα[174,175]. Putting these two observations together, it was hypothesized and demonstrated that RNA damage caused by UVB radiation or toxins activates the NLRP1 inflammasome through ZAKα; together with its downstream kinase p38, ZAKα directly phosphorylates a human-specific disordered linker region of NLRP1, leading to ubiquitylation and degradation of the NLRP1 N-terminus to activate the NLRP1 C-terminus. These data established inflammasome-driven pyroptosis as an integral component of the ribotoxic stress response[176,177]. Furthermore, the p38 kinase was implicated in mediating NLRP1 inflammasome activation after viral infection[176].

The 3C protease from human rhinoviruses, a type of picornavirus, and other proteases from diverse picornaviruses have been shown to cleave human NLRP1, resulting in its ubiquitylation via a cullin E3 ligase machinery and N-terminal degradation[178,179]. By contrast, viral dsRNA seems to activate human NLRP1 via a direct interaction independently of the proteasome[180]. NLRP1 is also emerging as a general sensor of cellular stress, including reductive stress, in which reduced thioredoxin-1 cannot bind to NLRP1 to restrain its activity[181,182], and protein folding stress, in which distinct inhibitors of protein folding or inducers of the unfolded protein response accelerate degradation of the N-terminal fragment of NLRP1 (ref. 183).

Structure of the NLRP1–DPP9 complex

DPP8 and DPP9 inhibit both rodent and human NLRP1 inflammasomes through a direct interaction with NLRP1 FIIND[171] (Fig. 4a). Cryo-EM structures of human or rat NLRP1 in complex with DPP9 surprisingly revealed a tripartite assembly, in which each DPP9 molecule of a DPP9 dimer binds one full-length NLRP1 and one UPA–CARD C-terminal fragment of NLRP1 (refs. 184,185) (Fig. 4b). Because these complexes were obtained from co-expression of NLRP1 and DPP9 in the absence of any stimulation, the existence of the UPA–CARD fragment suggests that it was generated either by increased degradation of the NLRP1 N-terminal fragment owing to overexpression-induced stress or by basal levels of N-terminal degradation during homoeostatic protein turnover.

In both structures, only the FIIND (ZU5 and UPA) of full-length NLRP1 and the UPA of the C-terminal fragment are visible, indicating that the remaining domains are flexibly linked[184,185]. In the FIIND of full-length NLRP1, ZU5 and UPA subdomains associate extensively with each other along the longer dimensions of their β-sandwich folds[184,185], illustrating how the N-terminal and C-terminal fragments in autoprocessed NLRP1 do not dissociate (Fig. 4b) until the N-terminal fragment is degraded by the proteasome. The FIIND of full-length NLRP1 can interact with DPP9 in the absence of the C-terminal UPA–CARD fragment, whereas the recruitment of the C-terminal UPA to DPP9 requires that DPP9 is already in complex with FIIND, and UPA alone cannot stably interact with DPP9 (refs. 184,185). In the human NLRP1–DPP9 complex, the N-terminal strand of the UPA of the C-terminal fragment of NLRP1, which contains a DPP9 substrate motif, inserts into the active-site tunnel of DPP9 to reach close to the active site, which is an interaction that is crucial for the recruitment of DPP9 (ref. 185). However, when the DPP9 inhibitor VbP is present, it binds in the active-site pocket of DPP9 to displace the UPA N-terminal strand from DPP9, resulting in release of the UPA–CARD fragment[185] (Fig. 4c).

These structures offer a plausible mechanism to explain how the tripartite NLRP1–DPP9 assembly inhibits the C-terminal fragment of NLRP1 from assembling an inflammasome. As shown below, the UPA of NLRP1 C-terminal fragment can self-oligomerize, which promotes CARD filament formation and inflammasome activation[71,72]. By contrast, DPP9-bound UPA is inhibited from oligomerization by steric hindrance (Fig. 4b), quenching the intrinsic ability of NLRP1 C-terminal fragment to form an inflammasome and avoiding inappropriate NLRP1 inflammasome activation during homoeostatic protein turnover that results in degradation of the N-terminal fragment of NLRP1. The structures imply that such inhibition requires that the concentration of full-length NLRP1 is greater than or equal to the concentration of C-terminal fragment. However, when NLRP1 is stimulated to undergo functional degradation, the amount of C-terminal fragment ultimately exceeds the amount of full-length NLRP1, leading to the accumulation of free C-terminal fragment. The C-terminal UPA and CARD then cooperatively oligomerize, which leads to CARD filament formation and inflammasome activation[71,72] (Fig. 4d,e).

Germline mutations of human NLRP1, which is expressed at high levels in human keratinocytes, lead to skin-related inflammatory diseases such as multiple self-healing palmoplantar carcinoma, familial keratosis lichenoides chronica[156], vitiligo[186,187] and autoinflammation with arthritis and dyskeratosis[171,188]. Among these deleterious mutations, A54T, A66V, M77T (ref. 156), L155H (refs. 186,187), R726W (ref. 188), ΔF787–R843 (ref. 156) and M1184V (refs. 186) lie in the autoinhibitory N-terminal fragment, whereas P1214R (refs. 171,188) localizes at the DPP9 substrate motif of the inflammatory C-terminal fragment, causing constitutive human NLRP1 activation and downstream pyroptosis[156,171] (Fig. 4a). Thus, the structural framework of the tripartite NLRP1–DPP9 assembly also helps to explain the biology of disease-associated NLRP1 mutations.

Structure of the NLRP1 C-terminal filament

The CARD of NLRP1 interacts with ASC, which bridges NLRP1 and caspase-1 for inflammasome assembly[189]. Previously determined CARD filament structures of the inflammasome components ASC, caspase-1 and NLRC4 (refs. 66,67) illustrated the mechanistic basis for self-oligomerization and hetero-oligomerization of CARDs. For NLRP1, an important distinguishing feature is that its CARD is ineffective in oligomerization by itself but can be promoted to oligomerize by the UPA domain[71,72]. Cryo-EM structures of the NLRP1 C-terminal fragment revealed an ordered density only for the CARDs, whereas oligomerized UPA molecules tend to be flexibly linked at the outside of the filament[71,72] (Fig. 4d). Unlike any of the other CARD filament structures solved previously, the NLRP1 C-terminal filament is composed of CARD dimers with twofold symmetry, rather than monomers, despite having similar helical symmetry to the other CARD filaments[72]. This CARD dimer structure was also observed in a previous crystal structure of NLRP1 (ref. 190). The dimer composition of the NLRP1 C-terminal assembly results in a two-layered appearance whereby the dimeric partners protrude outwards from the core filament[72] (Fig. 4d). However, the NLRP1 CARD assembly that is formed at high concentration and in the absence of UPA has a monomeric CARD filament[71], and the functional significance of the CARD dimer remains unclear.

Furthermore, the structures of NLRP1 UPA–CARD and NLRP1 CARD filaments predicted that the CARD of NLRP1 recruits the CARD of ASC through charge complementarity on the cross sections of

the filaments[71,72]. By contrast, NLRP1 CARD was predicted not to be able to recruit the CARD of caspase-1 directly owing to lack of structural and charge compatibility at the interface. The nature of UPA oligomerization was implicated by mutations at the interface between the UPAs of full-length NLRP1 and of the C-terminal fragment, which – despite the release of the C-terminal fragment from the tripartite NLRP1–DPP9 assembly – did not activate but rather abrogated inflammasome activation[185]. These data suggest that abrogation of inflammasome activation by the UPA mutations was owing to impaired UPA oligomerization through a mode of interaction observed in tripartite NLRP1–DPP9 (refs. 71,72,184,185).

Structure of the CARD8 inflammasome

Similar to NLRP1, human CARD8 (not present in rodents) has an autoproteolytic FIIND at its core – in addition to a disordered N-terminal region that varies between isoforms and a C-terminal CARD[162,191] – and has a similar mechanism of activation[162,170,191]. The inflammatory UPA–CARD C-terminal fragment of CARD8 must be released from the inhibitory N-terminal fragment to allow for CARD8 activation[170]. DPP8 and DPP9 directly interact with full-length CARD8 and the C-terminal fragment to suppress inflammasome activation during homoeostatic CARD8 turnover[192]. Small-molecule inhibitors of DPP8 and DPP9 induce pyroptosis in human monocytes and macrophages through CARD8 activation and are being investigated for potential cancer therapies[169,170]. CARD8 was shown to be an inflammasome sensor for HIV-1 protease, leading to CARD8 ubiquitylation, degradation of the N-terminal fragment and activation of the C-terminal fragment in infected cells[193]. In addition, anti-HIV-1 non-nucleoside reverse transcriptase inhibitors can promote premature activation of HIV-1 protease to trigger the CARD8 inflammasome, which suggests that targeting the CARD8 inflammasome could be a potent and broadly effective strategy for HIV eradication[193]. Proteases from diverse coronaviruses including SARS-CoV-2 (ref. 194) and enteroviruses[195] can also cleave CARD8, resulting in virus-induced pyroptosis in infected $CD4^+$ T cells, monocytes, macrophages or endothelial cells.

A cryo-EM structure of the CARD8–DPP9 complex has revealed regulatory mechanisms that are similar to those of NLRP1 (ref. 192). These mechanisms include the suppression of CARD8 C-terminal activity by DPP9 and full-length CARD8, the association of the N-terminal fragment with the C-terminal fragment in full-length CARD8, and the inhibition of CARD8 UPA oligomerization by the tripartite CARD8–DPP9 assembly[192]. However, in contrast to NLRP1, the N-terminal strand of CARD8 UPA alone does not insert deeply into the DPP9 active site and VbP does not directly displace CARD8 from DPP9 (ref. 192). Thus, it seems that VbP induces CARD8 activation mainly by proteostatic stress that upregulates CARD8 functional degradation.

Effects of inflammasome signalling

GSDMD was identified as a bona fide substrate for the inflammatory caspases through genetic screens, and the cleavage of human GSDMD at Asp275 generates an active N-terminal fragment and an autoinhibitory C-terminal fragment[37–39] (Fig. 5a,b). GSDMD had also previously been identified as a major hit for substrates of inflammatory caspases from a proteomics screen[196]. In addition to inflammasome-mediated cleavage, GSDMD can also be cleaved and activated by caspase-8, as well as by neutrophil granule enzymes[92,197,198]. GSDMD cleavage and activation are important for both the induction of pyroptosis and the release of IL-1 family cytokines from cells. The N-terminal fragment of GSDMD was shown to bind acidic lipids at the inner leaflet of plasma membranes and at mitochondrial membranes, and to mediate the formation of large transmembrane pores[40–45], providing a potential mechanistic basis for cytokine release through the pores and for membrane damage in pyroptosis[199,200]. Expression of GSDMD N-terminal fragment in human cells[40–45] and treatment of bacteria with recombinant N-terminal frgament[42] both caused cell death, indicating that the GSDMD N-terminal fragment has cytotoxic function. GSDMD belongs to a family of gasdermins and the discovery of their pore-forming activity redefined pyroptosis as gasdermin-mediated programmed lytic cell death[34,201]. This definition has now been extended by the role of NINJ1 in rupturing membranes to complete pyroptosis[202].

Structure of autoinhibited GSDMD

The mechanism of GSDMD autoinhibition has been indicated by crystal structures of full-length mouse GSDMA3 and full-length mouse and human GSDMD[41,203]. Even though extensive loop truncations were required for crystallization of GSDMD, the structures of truncated GSDMD nonetheless revealed that, similar to the GSDMA3 structure, the N-terminal fragment is composed of a twisted β-sheet surrounded by α-helices and a largely disordered region responsible for membrane insertion, and the C-terminal fragment is composed of tightly packed α-helices (Fig. 5b). The N-terminal and C-terminal fragments interact extensively to exert autoinhibition by masking membrane-binding elements. Disease-associated, gain-of-function mutations in GSDMD often map to the C-terminal fragment at the autoinhibitory contact sites; these mutations bypass signal-dependent activation of GSDMD and lead to its constitutive activation[41,203].

GSDMD is a substrate for all inflammatory caspases. The crystal structure of caspase-1 in complex with a GSDMD IDL peptide containing the FLTD tetrapeptide motif (residues 272–275 in human GSDMD) at first suggested that caspase-1 recognizes GSDMD using the same mechanism by which caspases self-cleave[204]. However, GSDMD recognition by inflammatory caspases turned out to be more complex. Biochemical and functional characterization revealed that caspase-4 and caspase-11 first need to be fully autoprocessed to generate the p10 fragment that participates in the active enzyme. A region of the caspases away from the active site (the exosite) then interacts with GSDMD C-terminal fragment with high affinity through hydrophobic and hydrogen-bonding interactions[205]. The exosite interaction positions the interdomain cleavage site of GSDMD at the caspase catalytic site, as shown by the crystal structure of caspase-1 in complex with full-length GSDMD[206] (Fig. 5c). This two-site mode of interaction has now also been observed in the structures of caspase-4 in complex with pro-IL-18 (refs. 89,90), which could suggest a general mechanism of substrate recognition by inflammatory caspases and could explain why inflammatory caspases seem to have fewer substrates than apoptotic caspases.

Structure of the GSDMD pore

The first gasdermin N-terminal structure in the pore form was revealed by cryo-EM studies of the GSDMA3 N-terminal pore, which showed the β-barrel nature of the pore, the large conformational changes that occur upon membrane insertion, and the mechanisms of lipid binding and oligomerization, with implications for the entire gasdermin family[207]. Recently, the human GSDMD N-terminal pore structure[33] was solved (Fig. 5d,e). In addition to fully formed pores with the large β-barrel that should traverse the membrane, these structures also revealed oligomerized rings without the β-barrel, which were dubbed 'prepores'[41,207]. The existence of a prepore structure suggests that it

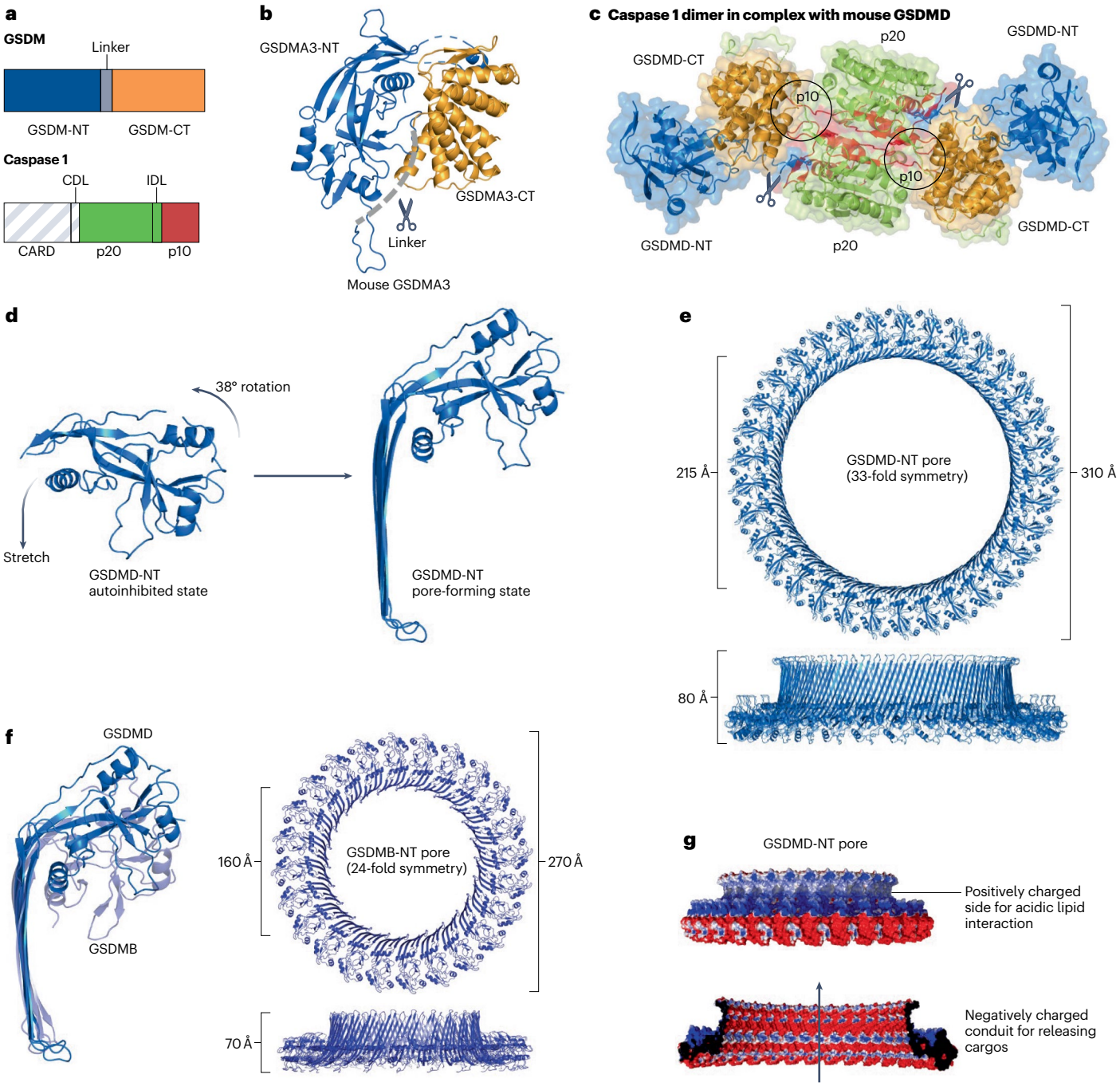

Fig. 5 | Gasdermins. a, Domain architectures of a gasdermin and caspase-1. Domains that are shown in grey indicate that the structure of this specific region is not shown in parts **b**–**g**. **b**, A gasdermin molecule, represented using the structure of mouse GSDMA3 [PDB:5B5R]. The scissor icon shows the interdomain cleavage site of gasdermin. **c**, The structure of caspase-1 p20/p10 dimer in complex with GSDMD [PDB:6VIE and 6KMV]. The active sites are marked as scissor icons, and the exosites are marked by circles. **d**, The structural changes of a human GSDMD N-terminal subunit from autoinhibited state [PDB:6N9O] to pore-forming state [PDB:6VFE], which could occur during prepore to pore transition on the membrane. The pore-forming state of GSDMD N-terminal fragment looks like a stretched hand; as the 'fingers' stretch out to form the transmembrane β-barrel, the globular domain undergoes a 38° rotation. **e**, The structure of a 33-subunit GSDMD N-terminal pore viewed from two orientations [PDB:6VFE]. **f**, Superposition of human GSDMD (blue) and human GSDMB (purple; [PDB:8ET2 and 8GTN]) pore-forming subunits and the structure of a 24-subunit GSDMB N-terminal pore viewed from two orientations [PDB:8ET2]. **g**, Electrostatic surface of the GSDMD pore viewed from outside and inside [PDB:6VFE]. The GSDMD membrane-binding regions are positively charged (blue), whereas the GSDMD conduit is negatively charged (red). The cargo release route is marked by an arrow. For parts **b**–**f**, domains are colour coded as in part **a**. CDL, CARD linker; CT, C-terminus; IDL, interdomain linker; NT, N-terminus.

may represent an oligomerized intermediate structure on membrane before GSDMD insertion and pore formation, but studies using atomic force microscopy have also suggested the assembly of arc-shaped and slit-shaped membrane pores that can transform into ring-shaped pores, which implies that further oligomerization can occur even after GSDMD membrane insertion[208].

Most GSDMA3 and GSDMD N-terminal pores reconstituted in vitro consist of 26–28 subunits and 31–34 subunits, respectively, with outer diameters of approximately 30 nm and inner diameters of approximately 20 nm. The membrane-inserted N-terminal fragment assumes the shape of a hand, with the membrane-binding α1 helix as a folded thumb, the rest of the globular region as the palm and two β-hairpins as the fingers. In autoinhibited full-length structures or prepores, the fingers of the N-terminal subunits are tucked into a fist and not extended. Thus, the main conformational change that occurs during membrane insertion involves the extension of the fingers to form the transmembrane β-barrel (Fig. 5d), whereas the globular domain faces the cytosol[33]. Pore structures for GSDMB N-terminal fragments have also been determined[209,210] (Fig. 5f), and a structural comparison suggests that the main differences between the different pore structures may occur at their lipid-binding elements.

The cryo-EM structure of the GSDMD pore[33] provided a plausible explanation as to why inflammasome-activated live cells release mature IL-1β or IL-18 protein but not their pro-IL precursors[211]. This is important because only the mature, processed cytokines can interact with their respective receptors to activate downstream gene expression and amplify inflammation. It was noted that although pro-IL-1β and pro-IL-18 are small in size relative to the inner dimension of the GSDMD pore, they are highly negatively charged (acidic) owing to their prodomains[35]. The GSDMD pore conduit is highly negatively charged (Fig. 5g), which suggested that it might repel negatively charged pro-IL-1β and pro-IL-18 to inhibit their release through the pore, through a mechanism known as electrostatic filtering[33]. Indeed, small negatively charged dextran or protein has the slowest rate of release from GSDMD pores relative to neutral or positively charge cargoes of similar molecular weights[33]. Mutating away acidic patches in the GSDMD N-terminal conduit compromised the selectivity of the pore against an acidic, negatively charged cargo[33,212]. Previously, unconventional secretion of fibroblast growth factor 2 (FGF2) was shown to depend on caspase-1 activity[213], raising the possibility that the highly basic (positively charged) protein FGF2 can be released from cells through caspase-1-activated GSDMD pores.

Interestingly, molecular modelling and calculations of electrostatic surface potential suggested that the acidic nature of the GSDMD pore conduit is conserved in other gasdermin pores[33], which raises the question of whether there are biological reasons to deter the release of a negatively charged cargo in general while allowing the release of a neutral or positively charged cargo. Certain other IL-1 family members, for example, IL-1α and IL-37, also have an acidic prodomain and become more basic upon maturation, which suggests that the mature forms of these cytokines might also be selectively released by gasdermin pores in live cells. In this context, and for another gasdermin family member GSDME, it was shown that T helper 17 cells activate NLRP3 to result in caspase-8 and caspase-3 activation, leading to GSDME cleavage[214]. GSDME pores, which also have an acidic conduit[33], then release mature IL-1α, processed by the calcium-activated cytosolic enzyme calpain, but not pro-IL-1α (ref. 214). Thus, although pro-IL-1α and IL-1α can both bind and activate the cognate receptor, in this case, only mature IL-1α is released and able to activate the receptor.

Structure of NINJ1 oligomers

The ninjurin proteins, including NINJ1 and its homologue NINJ2, are small cell-surface proteins first identified as adhesion molecules that promote axonal growth upon nerve injury[215,216]. NINJ1 (but not NINJ2) was later shown to mediate plasma membrane rupture downstream of GSDMD pore formation to complete lytic cell death[202]. The signal delivered by GSDMD to activate NINJ1 is currently unknown, but is likely to involve membrane permeabilization, membrane tension or membrane lipid redistribution, as NINJ1 is also activated by secondary necrosis, another lytic form of cell death[202]. Both NINJ1 and NINJ2 have a predicted domain architecture comprising an N-terminal segment that is important for cell adhesion, an amphipathic helix and two transmembrane helices at the C-terminal end[202] (Fig. 6a).

Structural studies have begun to reveal how NINJ1 may induce plasma membrane rupture. A recent cryo-EM study at a 3.8-Å resolution has shown that NINJ1 forms straight filaments, with one side being hydrophobic and the other side being hydrophilic[217]. In this structure, two NINJ1 filaments are bundled in the overall structure, with the hydrophobic faces of the filaments facing each other (Fig. 6b). Within each NINJ1 subunit, the predicted amphipathic extracellular helix actually comprises two helices (α1 and α2), followed by the transmembrane

Glossary

Alarmin
Alarmins are proteins, peptides, metabolites or others that are released to the outside of a cell in response to immune activation, as a result of transmembrane pore formation, cell injury and lytic death, or degranulation. These endogenous molecules may have chemotactic and/or immune-activating properties to alert the host for defence.

Cryopyrin-associated periodic syndromes
(CAPS). A set of genetic diseases of differing severity caused by autosomal dominant mutations in *NLRP3*. Patients with CAPS develop spontaneous inflammation and excessive release of the cytokine IL-1β, and may also suffer from arthralgia, deafness and hives.

Microtubule-organizing centre
(MTOC). A structure in eukaryotic cells from which microtubules are nucleated and emanate, which is often synonymous with the centrosome.

Neutrophil extracellular traps
Web-like networks of extracellular DNA, histones and neutrophil granule proteins extruded by neutrophils to trap and damage pathogens.

Pyroptosis
Programmed lytic cell death mediated by cleavage of gasdermin D by caspase-1, caspase-4, caspase-5 and caspase-11, or by other gasdermin family members, that occurs downstream of inflammasome activation or other insults.

Ribotoxic stress response
Activation of stress-associated kinases such as p38 and JNK1 owing to functional ribosome defects that result in inhibition or partial inhibition of protein translation. Downstream signalling can trigger cell cycle arrest, cell death and cytokine production.

Type III secretion
A bacterial secretion system involving a needle-like protein complex used to deliver effector proteins into the host cell cytosol; often found in pathogenic Gram-negative bacteria.

Unfolded protein response
A stress response resulting from the accumulation of unfolded or misfolded proteins in the endoplasmic reticulum that helps cells to reduce the stress through translation suppression, protein degradation and production of chaperones, or that induces cell death with prolonged stress.

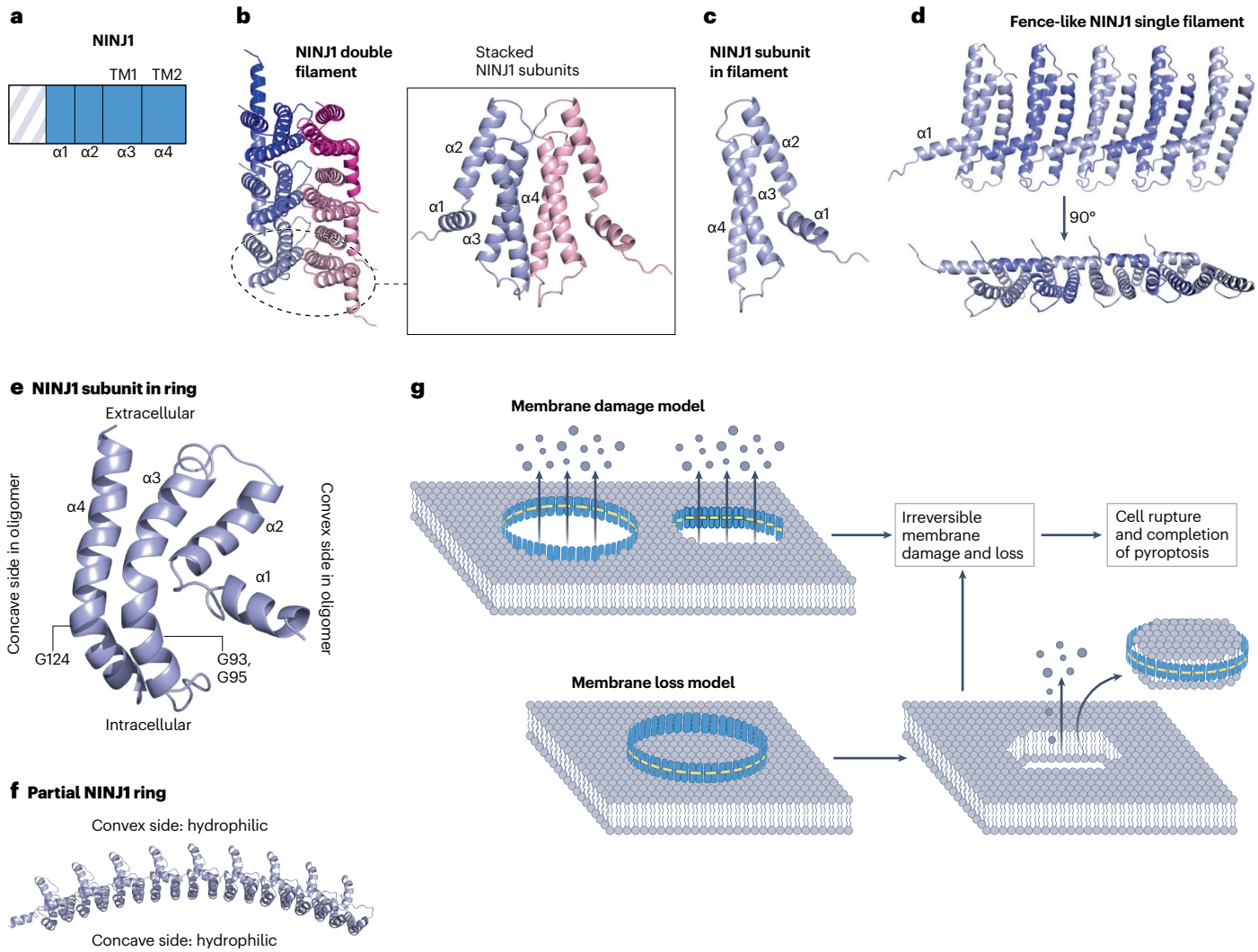

Fig. 6 | NINJ1. a, Domain architecture of ninjurin 1 (NINJ1). The domain shown in grey indicates that the structure of this specific region is not shown in parts **b**–**f**. **b**, Structural presentations of a NINJ1 double filament [PDB:8CQR] (left) and two stacked NINJ1 subunits (right). The double filament contains six subunits each with a different shade of blue or pink. Secondary structures are labelled for the blue subunit to the right. **c**, Structure of a single NINJ1 subunit. **d**, A single filament of five NINJ1 subunits (modelled from [PDB:8CQR]), in two orientations. The α1 helix of one subunit extends over to the transmembrane helices α3 and α4 of a neighbouring subunit to make a NINJ1 chain. **e**, Structural representation of a NINJ1 subunit from rings or curved filaments, showing bent helices α3 and α4. **f**, A model of a partial NINJ1 ring built by propagating the NINJ1 segment structure, showing the concave hydrophobic side and the convex hydrophilic side. **g**, Two alternative models of NINJ1 activation: the membrane damage model, in which NINJ1 filaments or pores cause membrane leakage, and the membrane loss model, in which NINJ1 assembles around a patch of membrane, leading to its release. In both models, the α1 and α2 subunits of NINJ1 (shown in yellow) directly cause membrane damage. TM, transmembrane helix.

helices (α3 and α4) that form a hairpin within the membrane (Fig. 6c). In each single filament, the α3–α4 hairpin of one NINJ1 subunit interacts side-by-side with that of a neighbouring subunit to form a chain assembly in the shape of a fence, within which each α1 helix crosses over to the neighbouring subunit to stabilize the assembly (Fig. 6d). The extreme N-terminal region is disordered in this structure. This structure and molecular dynamic simulations led to the hypothesis that the NINJ1 single filament with a hydrophilic side and a hydrophobic side can stably cap membrane edges or form large transmembrane pores. Thus, during lytic cell death, the extracellular helices insert into the plasma membrane to polymerize NINJ1 monomers and rupture the plasma membrane.

Two preprints reporting structural, biochemical and cell biological studies of NINJ1 now add further mechanistic insights into the ability of NINJ1 oligomers to rupture the membrane. In one of the preprints, both NINJ1 and NINJ2 structures were solved by cryo-EM as bundled double filaments at a 2.8-Å and a 3.1-Å resolution, respectively[218]. These structures are similar to that previously published[217] and were proposed to have been formed during the purification process by the bound lipids as almost no protein–protein interactions exist between the filaments and some single NINJ1 filaments were also observed under cryo-EM[218]. In the other preprint, curved filaments and ring-shaped oligomers of NINJ1 were observed in detergents, and when reconstituted with

liposomes, NINJ1, but not NINJ2, was shown to 'dissolve' liposomes, leaving small heterogeneous rings and larger patches[219]. Cryo-EM reconstruction using short segments from these rings and filaments (approximately six subunits), reaching a 4.3-Å resolution, revealed a similar fence-like assembly but with a few differences. At the level of individual NINJ1 subunits, instead of being straight, the α3 and α4 helices are highly bent, with Gly residues at the kinks in both helices (Fig. 6e). At the level of NINJ1 filaments, instead of being straight (Fig. 6b), there is a prominent curvature on the plane of the assembly, with the concave side being hydrophobic and the convex side being hydrophilic (Fig. 6f). The degree of this curvature can vary owing to the intrinsic plasticity of the subunit interactions, but the hydrophobic side, which seems to be denser owing to the fence-like helices, always faces the concave side[219].

These studies have begun to suggest intriguing mechanisms for NINJ1-mediated membrane rupture. The published structure[217] proposes a 'membrane damage' model in which the amphipathic single filaments could promote membrane rupture by capping and stabilizing membrane lesions of variable sizes to allow the release of DAMPs, or proposes that NINJ1 double filaments could open up into pores in response to osmotic pressure to form membrane lesions (Fig. 6g). The two preprints[218,219] propose a 'membrane loss' model in which NINJ1 oligomers could break membrane and solubilize membrane patches by encircling them, acting as membrane scaffolding proteins in nanodiscs (Fig. 6g). The latter model is supported by the hydrophobicity of the concave side of NINJ1 oligomers[219] and by the observed release of NINJ1 oligomers into the cell culture medium[218,219]. In either model, the amphipathic nature of the NINJ1 oligomeric structure is key. When the rate of membrane damage exceeds that of membrane repair, or in the case of the membrane loss model when there is also insufficient membrane to patch up the damage, complete membrane rupture may ensue to release alarmins of different sizes. Although changes in membrane tension and/or lipid composition have been proposed to trigger NINJ1 activation, what exactly activates NINJ1 and how this occurs remain to be elucidated. In addition, the features of NINJ1, but not NINJ2, that determine its function in cell killing remain to be fully addressed.

Conclusions and future directions

In this Review, we present a structural and mechanistic view of inflammasomes, from how the sensor proteins are autoinhibited, regulated and activated to assemble with adaptor proteins and effector caspases to how the effector proteins (caspases, gasdermins and NINJ1) are activated to execute their functions in cytokine release and cell death. We anticipate that future structural information will further elucidate the complex regulatory network of the well-studied inflammasomes discussed here, provide a first glimpse as to the mechanisms of understudied inflammasomes, and reveal new therapeutic targets and their structural templates to tackle the large number of inflammasomopathies.

Published online: 19 February 2024

References

1. Lomedico, P. T. et al. Cloning and expression of murine interleukin-1 cDNA in *Escherichia coli*. *Nature* **312**, 458–462 (1984).
2. Auron, P. E. et al. Nucleotide sequence of human monocyte interleukin 1 precursor cDNA. *Proc. Natl Acad. Sci. USA* **81**, 7907–7911 (1984).
3. Van Damme, J. et al. Homogeneous interferon-inducing 22K factor is related to endogenous pyrogen and interleukin-1. *Nature* **314**, 266–268 (1985).
4. Cerretti, D. P. et al. Molecular cloning of the interleukin-1 beta converting enzyme. *Science* **256**, 97–100 (1992).
5. Thornberry, N. A. et al. A novel heterodimeric cysteine protease is required for interleukin-1 beta processing in monocytes. *Nature* **356**, 768–774 (1992).
6. Nicholson, D. W. Caspase structure, proteolytic substrates, and function during apoptotic cell death. *Cell Death Differ.* **6**, 1028–1042 (1999).
7. Shalini, S., Dorstyn, L., Dawar, S. & Kumar, S. Old, new and emerging functions of caspases. *Cell Death Differ.* **22**, 526–539 (2015).
8. Man, S. M. & Kanneganti, T. D. Converging roles of caspases in inflammasome activation, cell death and innate immunity. *Nat. Rev. Immunol.* **16**, 7–21 (2016).
9. Martinon, F., Burns, K. & Tschopp, J. The inflammasome: a molecular platform triggering activation of inflammatory caspases and processing of proIL-beta. *Mol. Cell* **10**, 417–426 (2002).
This paper identifies a molecular complex that activates caspase-1, which was termed the inflammasome.
10. Feldmann, J. et al. Chronic infantile neurological cutaneous and articular syndrome is caused by mutations in CIAS1, a gene highly expressed in polymorphonuclear cells and chondrocytes. *Am. J. Hum. Genet.* **71**, 198–203 (2002).
11. Hoffman, H. M., Mueller, J. L., Broide, D. H., Wanderer, A. A. & Kolodner, R. D. Mutation of a new gene encoding a putative pyrin-like protein causes familial cold autoinflammatory syndrome and Muckle-Wells syndrome. *Nat. Genet.* **29**, 301–305 (2001).
12. Agostini, L. et al. NALP3 forms an IL-1beta-processing inflammasome with increased activity in Muckle-Wells autoinflammatory disorder. *Immunity* **20**, 319–325 (2004).
13. Martinon, F., Petrilli, V., Mayor, A., Tardivel, A. & Tschopp, J. Gout-associated uric acid crystals activate the NALP3 inflammasome. *Nature* **440**, 237–241 (2006).
14. So, A., De Smedt, T., Revaz, S. & Tschopp, J. A pilot study of IL-1 inhibition by anakinra in acute gout. *Arthritis Res. Ther.* **9**, R28 (2007).
15. Hawkins, P. N., Lachmann, H. J., Aganna, E. & McDermott, M. F. Spectrum of clinical features in Muckle-Wells syndrome and response to anakinra. *Arthritis Rheum.* **50**, 607–612 (2004).
16. Jin, T. et al. Structures of the HIN domain:DNA complexes reveal ligand binding and activation mechanisms of the AIM2 inflammasome and IFI16 receptor. *Immunity* **36**, 561–571 (2012).
17. Matyszewski, M. et al. Distinct axial and lateral interactions within homologous filaments dictate the signaling specificity and order of the AIM2-ASC inflammasome. *Nat. Commun.* **12**, 2735 (2021).
18. Jin, T., Perry, A., Smith, P., Jiang, J. & Xiao, T. S. Structure of the absent in melanoma 2 (AIM2) pyrin domain provides insights into the mechanisms of AIM2 autoinhibition and inflammasome assembly. *J. Biol. Chem.* **288**, 13225–13235 (2013).
19. Lu, A. et al. Plasticity in PYD assembly revealed by cryo-EM structure of the PYD filament of AIM2. *Cell Discov.* **1**, 15013 (2015).
20. Weinert, C., Morger, D., Djekic, A., Grutter, M. G. & Mittl, P. R. Crystal structure of TRIM20 C-terminal coiled-coil/B30.2 fragment: implications for the recognition of higher order oligomers. *Sci. Rep.* **5**, 10819 (2015).
21. Shen, C. et al. Phase separation drives RNA virus-induced activation of the NLRP6 inflammasome. *Cell* **184**, 5759–5774 (2021).
22. Barnett, K. C., Li, S., Liang, K. & Ting, J. P. A 360 degrees view of the inflammasome: mechanisms of activation, cell death, and diseases. *Cell* **186**, 2288–2312 (2023).
23. Broz, P. & Dixit, V. M. Inflammasomes: mechanism of assembly, regulation and signalling. *Nat. Rev. Immunol.* **16**, 407–420 (2016).
24. Rathinam, V. A. & Fitzgerald, K. A. Inflammasome complexes: emerging mechanisms and effector functions. *Cell* **165**, 792–800 (2016).
25. Mangan, M. S. J. et al. Targeting the NLRP3 inflammasome in inflammatory diseases. *Nat. Rev. Drug Discov.* **17**, 688 (2018).
26. Schroder, K. & Tschopp, J. The inflammasomes. *Cell* **140**, 821–832 (2010).
27. Fu, J. & Wu, H. Structural mechanisms of NLRP3 inflammasome assembly and activation. *Annu. Rev. Immunol.* **41**, 301–316 (2023).
28. Swanson, K. V., Deng, M. & Ting, J. P. The NLRP3 inflammasome: molecular activation and regulation to therapeutics. *Nat. Rev. Immunol.* **19**, 477–489 (2019).
29. Chan, A. H. et al. Caspase-4 dimerisation and D289 auto-processing elicit an interleukin-1beta-converting enzyme. *Life Sci. Alliance* **6**, e202301908 (2023).
30. Wandel, M. P. et al. Guanylate-binding proteins convert cytosolic bacteria into caspase-4 signaling platforms. *Nat. Immunol.* **21**, 880–891 (2020).
31. Naseer, N. et al. *Salmonella enterica* serovar Typhimurium induces NAIP/NLRC4- and NLRP3/ASC-independent, caspase-4-dependent inflammasome activation in human intestinal epithelial cells. *Infect. Immun.* **90**, e0066321 (2022).
32. Knodler, L. A. et al. Noncanonical inflammasome activation of caspase-4/caspase-11 mediates epithelial defenses against enteric bacterial pathogens. *Cell Host Microbe* **16**, 249–256 (2014).
33. Xia, S. et al. Gasdermin D pore structure reveals preferential release of mature interleukin-1. *Nature* **593**, 607–611 (2021).
This paper reports the structure of the GSDMD pore and illustrates how the charge features in the pore conduit determine the electrostatic filtering that retains pro-IL-1b but releases mature IL-1b.
34. Liu, X., Xia, S., Zhang, Z., Wu, H. & Lieberman, J. Channelling inflammation: gasdermins in physiology and disease. *Nat. Rev. Drug Discov.* **20**, 384–405 (2021).
35. Monteleone, M. et al. Interleukin-1 beta maturation triggers its relocation to the plasma membrane for gasdermin-D-dependent and -independent secretion. *Cell Rep.* **24**, 1425–1433 (2018).
36. Cookson, B. T. & Brennan, M. A. Pro-inflammatory programmed cell death. *Trends Microbiol.* **9**, 113–114 (2001).
37. Shi, J. et al. Cleavage of GSDMD by inflammatory caspases determines pyroptotic cell death. *Nature* **526**, 660–665 (2015).

38. Kayagaki, N. et al. Caspase-11 cleaves gasdermin D for non-canonical inflammasome signalling. *Nature* **526**, 666–671 (2015).
39. He, W. T. et al. Gasdermin D is an executor of pyroptosis and required for interleukin-1beta secretion. *Cell Res.* **25**, 1285–1298 (2015).
40. Aglietti, R. A. et al. GsdmD p30 elicited by caspase-11 during pyroptosis forms pores in membranes. *Proc. Natl Acad. Sci. USA* **113**, 7858–7863 (2016).
41. Ding, J. et al. Pore-forming activity and structural autoinhibition of the gasdermin family. *Nature* **535**, 111–116 (2016).
42. Liu, X. et al. Inflammasome-activated gasdermin D causes pyroptosis by forming membrane pores. *Nature* **535**, 153–158 (2016).
43. Sborgi, L. et al. Structure and assembly of the mouse ASC inflammasome by combined NMR spectroscopy and cryo-electron microscopy. *Proc. Natl Acad. Sci. USA* **112**, 13237–13242 (2015).
44. Chen, X. et al. Pyroptosis is driven by non-selective gasdermin-D pore and its morphology is different from MLKL channel-mediated necroptosis. *Cell Res.* **26**, 1007–1020 (2016).
45. Russo, H. M. et al. Active caspase-1 induces plasma membrane pores that precede pyroptotic lysis and are blocked by lanthanides. *J. Immunol.* **197**, 1353–1367 (2016).
46. Zheng, D., Liwinski, T. & Elinav, E. Inflammasome activation and regulation: toward a better understanding of complex mechanisms. *Cell Discov.* **6**, 36 (2020).
47. Christgen, S., Place, D. E. & Kanneganti, T. D. Toward targeting inflammasomes: insights into their regulation and activation. *Cell Res.* **30**, 315–327 (2020).
48. Tanase, D. M. et al. Portrayal of NLRP3 inflammasome in atherosclerosis: current knowledge and therapeutic targets. *Int. J. Mol. Sci.* **24**, 8162 (2023).
49. Wang, Y., Sui, Z., Wang, M. & Liu, P. Natural products in attenuating renal inflammation via inhibiting the NLRP3 inflammasome in diabetic kidney disease. *Front. Immunol.* **14**, 1196016 (2023).
50. Tall, A. R. & Bornfeldt, K. E. Inflammasomes and atherosclerosis: a mixed picture. *Circ. Res.* **132**, 1505–1520 (2023).
51. Khanmohammadi, S., Ramos-Molina, B. & Kuchay, M. S. NOD-like receptors in the pathogenesis of metabolic (dysfunction)-associated fatty liver disease: therapeutic agents targeting NOD-like receptors. *Diabetes Metab. Syndr.* **17**, 102788 (2023).
52. Wang, M. et al. Inflammasomes: a rising star on the horizon of COVID-19 pathophysiology. *Front. Immunol.* **14**, 1185233 (2023).
53. Bauer, S., Hezinger, L., Rexhepi, F., Ramanathan, S. & Kufer, T. A. NOD-like receptors — emerging links to obesity and associated morbidities. *Int. J. Mol. Sci.* **24**, 8595 (2023).
54. Janeway, C. A. Jr. Approaching the asymptote? Evolution and revolution in immunology. *Cold Spring Harb. Symp. Quant. Biol.* **54**, 1–13 (1989).
55. Chou, W. C., Jha, S., Linhoff, M. W. & Ting, J. P. The NLR gene family: from discovery to present day. *Nat. Rev. Immunol.* **23**, 635–654 (2023).
56. Hornung, V. et al. AIM2 recognizes cytosolic dsDNA and forms a caspase-1-activating inflammasome with ASC. *Nature* **458**, 514–518 (2009).
57. Fernandes-Alnemri, T., Yu, J. W., Datta, P., Wu, J. & Alnemri, E. S. AIM2 activates the inflammasome and cell death in response to cytoplasmic DNA. *Nature* **458**, 509–513 (2009).
58. Heilig, R. & Broz, P. Function and mechanism of the pyrin inflammasome. *Eur. J. Immunol.* **48**, 230–238 (2018).
59. Lu, A. et al. Unified polymerization mechanism for the assembly of ASC-dependent inflammasomes. *Cell* **156**, 1193–1206 (2014).
This paper reports the first PYD filament structure and the nucleated polymerization mechanism for PYD and CARD in inflammasome assembly.
60. Richards, N. et al. Interaction between pyrin and the apoptotic speck protein (ASC) modulates ASC-induced apoptosis. *J. Biol. Chem.* **276**, 39320–39329 (2001).
61. Lu, A., Kabaleeswaran, V., Fu, T., Magupalli, V. G. & Wu, H. Crystal structure of the F27G AIM2 PYD mutant and similarities of its self-association to DED/DED interactions. *J. Mol. Biol.* **426**, 1420–1427 (2014).
62. Hochheiser, I. V. et al. Directionality of PYD filament growth determined by the transition of NLRP3 nucleation seeds to ASC elongation. *Sci. Adv.* **8**, eabn7583 (2022).
63. Shen, C. et al. Molecular mechanism for NLRP6 inflammasome assembly and activation. *Proc. Natl Acad. Sci. USA* **116**, 2052–2057 (2019).
64. Dick, M. S., Sborgi, L., Ruhl, S., Hiller, S. & Broz, P. ASC filament formation serves as a signal amplification mechanism for inflammasomes. *Nat. Commun.* **7**, 11929 (2016).
65. de Alba, E. Structure and interdomain dynamics of apoptosis-associated speck-like protein containing a CARD (ASC). *J. Biol. Chem.* **284**, 32932–32941 (2009).
66. Lu, A. et al. Molecular basis of caspase-1 polymerization and its inhibition by a new capping mechanism. *Nat. Struct. Mol. Biol.* **23**, 416–425 (2016).
67. Li, Y. et al. Cryo-EM structures of ASC and NLRC4 CARD filaments reveal a unified mechanism of nucleation and activation of caspase-1. *Proc. Natl Acad. Sci. USA* **115**, 10845–10852 (2018).
68. Stutz, A., Horvath, G. L., Monks, B. G. & Latz, E. ASC speck formation as a readout for inflammasome activation. *Methods Mol. Biol.* **1040**, 91–101 (2013).
69. Masumoto, J. et al. ASC, a novel 22-kDa protein, aggregates during apoptosis of human promyelocytic leukemia HL-60 cells. *J. Biol. Chem.* **274**, 33835–33838 (1999).
70. Moriya, M. et al. Role of charged and hydrophobic residues in the oligomerization of the PYRIN domain of ASC. *Biochemistry* **44**, 575–583 (2005).
71. Gong, Q. et al. Structural basis for distinct inflammasome complex assembly by human NLRP1 and CARD8. *Nat. Commun.* **12**, 188 (2021).
72. Hollingsworth, L. R. et al. Mechanism of filament formation in UPA-promoted CARD8 and NLRP1 inflammasomes. *Nat. Commun.* **12**, 189 (2021).
73. Zhang, L. et al. Cryo-EM structure of the activated NAIP2-NLRC4 inflammasome reveals nucleated polymerization. *Science* **350**, 404–409 (2015).
74. Wang, L., Sharif, H., Vora, S. M., Zheng, Y. & Wu, H. Structures and functions of the inflammasome engine. *J. Allergy Clin. Immunol.* **147**, 2021–2029 (2021).
75. Vance, R. E. The NAIP/NLRC4 inflammasomes. *Curr. Opin. Immunol.* **32**, 84–89 (2015).
76. Hu, Z. et al. Crystal structure of NLRC4 reveals its autoinhibition mechanism. *Science* **341**, 172–175 (2013).
This paper shows the structure of an autoinhibited NLRC4 monomer.
77. Hu, Z. et al. Structural and biochemical basis for induced self-propagation of NLRC4. *Science* **350**, 399–404 (2015).
Together with Zhang et al. (2015), this paper shows the structure of the active NLRC4 oligomer, revealing a nucleated polymerization mechanism in NLRC4 oligomerization.
78. Paidimuddala, B. et al. Mechanism of NAIP-NLRC4 inflammasome activation revealed by cryo-EM structure of unliganded NAIP5. *Nat. Struct. Mol. Biol.* **30**, 159–166 (2023).
This paper shows the structure of unliganded NAIP5, revealing how NLRC4 can be bound to NAIP5 before flagellin binding and how NLRC4 is activated conformationally upon flagellin binding.
79. Schmidt, F. I. et al. A single domain antibody fragment that recognizes the adaptor ASC defines the role of ASC domains in inflammasome assembly. *J. Exp. Med.* **213**, 771–790 (2016).
80. Man, S. M. et al. Inflammasome activation causes dual recruitment of NLRC4 and NLRP3 to the same macromolecular complex. *Proc. Natl Acad. Sci. USA* **111**, 7403–7408 (2014).
81. Broz, P., von Moltke, J., Jones, J. W., Vance, R. E. & Monack, D. M. Differential requirement for caspase-1 autoproteolysis in pathogen-induced cell death and cytokine processing. *Cell Host Microbe* **8**, 471–483 (2010).
82. Ross, C. et al. Inflammatory caspases: toward a unified model for caspase activation by inflammasomes. *Annu. Rev. Immunol.* **40**, 249–269 (2022).
83. Boucher, D. et al. Caspase-1 self-cleavage is an intrinsic mechanism to terminate inflammasome activity. *J. Exp. Med.* **215**, 827–840 (2018).
84. Shi, J. et al. Inflammatory caspases are innate immune receptors for intracellular LPS. *Nature* **514**, 187–192 (2014).
85. Kayagaki, N. et al. Non-canonical inflammasome activation targets caspase-11. *Nature* **479**, 117–121 (2011).
86. Zanoni, I. et al. An endogenous caspase-11 ligand elicits interleukin-1 release from living dendritic cells. *Science* **352**, 1232–1236 (2016).
87. Ross, C., Chan, A. H., Von Pein, J., Boucher, D. & Schroder, K. Dimerization and auto-processing induce caspase-11 protease activation within the non-canonical inflammasome. *Life Sci. Alliance* **1**, e201800237 (2018).
88. Lee, B. L. et al. Caspase-11 auto-proteolysis is crucial for noncanonical inflammasome activation. *J. Exp. Med.* **215**, 2279–2288 (2018).
89. Devant, P. et al. Structural insights into cytokine cleavage by inflammatory caspase-4. *Nature* https://doi.org/10.1038/s41586-023-06751-9 (2023).
90. Shi, X. et al. Recognition and maturation of IL-18 by caspase-4 noncanonical inflammasome. *Nature* https://doi.org/10.1038/s41586-023-06742-w (2023).
91. Gaidt, M. M. & Hornung, V. Pore formation by GSDMD is the effector mechanism of pyroptosis. *EMBO J.* **35**, 2167–2169 (2016).
92. Sollberger, G. et al. Gasdermin D plays a vital role in the generation of neutrophil extracellular traps. *Sci. Immunol.* **3**, eaar6689 (2018).
93. Chen, K. W. et al. Noncanonical inflammasome signaling elicits gasdermin D-dependent neutrophil extracellular traps. *Sci. Immunol.* **3**, eaar6676 (2018).
94. Yang, J., Zhao, Y., Shi, J. & Shao, F. Human NAIP and mouse NAIP1 recognize bacterial type III secretion needle protein for inflammasome activation. *Proc. Natl Acad. Sci. USA* **110**, 14408–14413 (2013).
95. Zhao, Y. et al. The NLRC4 inflammasome receptors for bacterial flagellin and type III secretion apparatus. *Nature* **477**, 596–600 (2011).
96. Kofoed, E. M. & Vance, R. E. Innate immune recognition of bacterial ligands by NAIPs determines inflammasome specificity. *Nature* **477**, 592–595 (2011).
97. Miao, E. A. et al. Innate immune detection of the type III secretion apparatus through the NLRC4 inflammasome. *Proc. Natl Acad. Sci. USA* **107**, 3076–3080 (2010).
98. Kortmann, J., Brubaker, S. W. & Monack, D. M. Cutting edge: inflammasome activation in primary human macrophages is dependent on flagellin. *J. Immunol.* **195**, 815–819 (2015).
99. Yang, X. et al. Structural basis for specific flagellin recognition by the NLR protein NAIP5. *Cell Res.* **28**, 35–47 (2018).
This paper reports the structure of NAIP5 in complex with flagellin and a mutant NLRC4 that cannot oligomerize, revealing how NAIP5 recognizes flagellin.
100. Tenthorey, J. L. et al. The structural basis of flagellin detection by NAIP5: a strategy to limit pathogen immune evasion. *Science* **358**, 888–893 (2017).
This paper reports the structure of NAIP5 in complex with flagellin and NLRC4, revealing how NAIP5 recognizes flagellin.
101. Sutterwala, F. S. et al. Critical role for NALP3/CIAS1/Cryopyrin in innate and adaptive immunity through its regulation of caspase-1. *Immunity* **24**, 317–327 (2006).
102. Franchi, L., Eigenbrod, T. & Nunez, G. Cutting edge: TNF-alpha mediates sensitization to ATP and silica via the NLRP3 inflammasome in the absence of microbial stimulation. *J. Immunol.* **183**, 792–796 (2009).
103. Bauernfeind, F. G. et al. Cutting edge: NF-kappaB activating pattern recognition and cytokine receptors license NLRP3 inflammasome activation by regulating NLRP3 expression. *J. Immunol.* **183**, 787–791 (2009).

104. McKee, C. M. & Coll, R. C. NLRP3 inflammasome priming: a riddle wrapped in a mystery inside an enigma. *J. Leukoc. Biol.* **108**, 937–952 (2020).
105. Hara, H. et al. The NLRP6 inflammasome recognizes lipoteichoic acid and regulates Gram-positive pathogen infection. *Cell* **175**, 1651–1664.e14 (2018).
106. Puren, A. J., Fantuzzi, G. & Dinarello, C. A. Gene expression, synthesis, and secretion of interleukin 18 and interleukin 1beta are differentially regulated in human blood mononuclear cells and mouse spleen cells. *Proc. Natl Acad. Sci. USA* **96**, 2256–2261 (1999).
107. Marshall, J. D. et al. Regulation of human IL-18 mRNA expression. *Clin. Immunol.* **90**, 15–21 (1999).
108. Juliana, C. et al. Non-transcriptional priming and deubiquitination regulate NLRP3 inflammasome activation. *J. Biol. Chem.* **287**, 36617–36622 (2012).
109. Py, B. F., Kim, M. S., Vakifahmetoglu-Norberg, H. & Yuan, J. Deubiquitination of NLRP3 by BRCC3 critically regulates inflammasome activity. *Mol. Cell* **49**, 331–338 (2013).
110. Xing, Y. et al. Cutting edge: TRAF6 mediates TLR/IL-1R signaling-induced nontranscriptional priming of the NLRP3 inflammasome. *J. Immunol.* **199**, 1561–1566 (2017).
111. Fernandes-Alnemri, T. et al. Cutting edge: TLR signaling licenses IRAK1 for rapid activation of the NLRP3 inflammasome. *J. Immunol.* **191**, 3995–3999 (2013).
112. Lin, K. M. et al. IRAK-1 bypasses priming and directly links TLRs to rapid NLRP3 inflammasome activation. *Proc. Natl Acad. Sci. USA* **111**, 775–780 (2014).
113. Song, N. et al. NLRP3 phosphorylation is an essential priming event for inflammasome activation. *Mol. Cell* **68**, 185–197.e6 (2017).
114. Perregaux, D. & Gabel, C. A. Interleukin-1 beta maturation and release in response to ATP and nigericin. Evidence that potassium depletion mediated by these agents is a necessary and common feature of their activity. *J. Biol. Chem.* **269**, 15195–15203 (1994).
115. Petrilli, V. et al. Activation of the NALP3 inflammasome is triggered by low intracellular potassium concentration. *Cell Death Differ.* **14**, 1583–1589 (2007).
116. Munoz-Planillo, R. et al. K^+ efflux is the common trigger of NLRP3 inflammasome activation by bacterial toxins and particulate matter. *Immunity* **38**, 1142–1153 (2013).
117. Mariathasan, S. et al. Cryopyrin activates the inflammasome in response to toxins and ATP. *Nature* **440**, 228–232 (2006).
118. Di, A. et al. The TWIK2 potassium efflux channel in macrophages mediates NLRP3 inflammasome-induced inflammation. *Immunity* **49**, 56–65.e4 (2018).
119. Murakami, T. et al. Critical role for calcium mobilization in activation of the NLRP3 inflammasome. *Proc. Natl Acad. Sci. USA* **109**, 11282–11287 (2012).
120. Katsnelson, M. A., Rucker, L. G., Russo, H. M. & Dubyak, G. R. K+ efflux agonists induce NLRP3 inflammasome activation independently of Ca2+ signaling. *J. Immunol.* **194**, 3937–3952 (2015).
121. Hornung, V. et al. Silica crystals and aluminum salts activate the NALP3 inflammasome through phagosomal destabilization. *Nat. Immunol.* **9**, 847–856 (2008).
122. Dostert, C. et al. Innate immune activation through Nalp3 inflammasome sensing of asbestos and silica. *Science* **320**, 674–677 (2008).
123. Duewell, P. et al. NLRP3 inflammasomes are required for atherogenesis and activated by cholesterol crystals. *Nature* **464**, 1357–1361 (2010).
124. Rajamaki, K. et al. Cholesterol crystals activate the NLRP3 inflammasome in human macrophages: a novel link between cholesterol metabolism and inflammation. *PloS ONE* **5**, e11765 (2010).
125. Halle, A. et al. The NALP3 inflammasome is involved in the innate immune response to amyloid-beta. *Nat. Immunol.* **9**, 857–865 (2008).
126. Dostert, C. et al. Malarial hemozoin is a Nalp3 inflammasome activating danger signal. *PloS ONE* **4**, e6510 (2009).
127. Shimada, K. et al. Oxidized mitochondrial DNA activates the NLRP3 inflammasome during apoptosis. *Immunity* **36**, 401–414 (2012).
128. Nakahira, K. et al. Autophagy proteins regulate innate immune responses by inhibiting the release of mitochondrial DNA mediated by the NALP3 inflammasome. *Nat. Immunol.* **12**, 222–230 (2011).
129. Zhong, Z. et al. New mitochondrial DNA synthesis enables NLRP3 inflammasome activation. *Nature* **560**, 198–203 (2018).
130. Xian, H. et al. Oxidized DNA fragments exit mitochondria via mPTP- and VDAC-dependent channels to activate NLRP3 inflammasome and interferon signaling. *Immunity* **55**, 1370–1385.e8 (2022).
131. Gross, C. J. et al. K^+ efflux-independent NLRP3 inflammasome activation by small molecules targeting mitochondria. *Immunity* **45**, 761–773 (2016).
132. Sharif, H. et al. Structural mechanism for NEK7-licensed activation of NLRP3 inflammasome. *Nature* **570**, 338–343 (2019).
This paper reports the structure of PYD-deleted NLRP3 in complex with NEK7.
133. He, Y., Zeng, M. Y., Yang, D., Motro, B. & Nunez, G. NEK7 is an essential mediator of NLRP3 activation downstream of potassium efflux. *Nature* **530**, 354–357 (2016).
134. Schmid-Burgk, J. L. et al. A genome-wide CRISPR (clustered regularly interspaced short palindromic repeats) screen identifies NEK7 as an essential component of NLRP3 inflammasome activation. *J. Biol. Chem.* **291**, 103–109 (2016).
135. Shi, H. et al. NLRP3 activation and mitosis are mutually exclusive events coordinated by NEK7, a new inflammasome component. *Nat. Immunol.* **17**, 250–258 (2016).
136. Coll, R. C. et al. A small-molecule inhibitor of the NLRP3 inflammasome for the treatment of inflammatory diseases. *Nat. Med.* **21**, 248–255 (2015).
137. Schmacke, N. A. et al. IKKβ primes inflammasome formation by recruiting NLRP3 to the trans-Golgi network. *Immunity* **55**, 2271–2284.e7 (2022).
138. Xiao, L., Magupalli, V. G. & Wu, H. Cryo-EM structures of the active NLRP3 inflammasome disc. *Nature* **613**, 595–600 (2023).
This paper reports the NLRP3–NEK7–ASC inflammasome disc in active form, showing the ATP-induced conformational changes.
139. Hochheiser, I. V. et al. Structure of the NLRP3 decamer bound to the cytokine release inhibitor CRID3. *Nature* **604**, 184–189 (2022).
This paper reports the structure of full-length human NLRP3 in a decameric form in complex with the NLRP3 inhibitor CRID3.
140. Andreeva, L. et al. NLRP3 cages revealed by full-length mouse NLRP3 structure control pathway activation. *Cell* **184**, 6299–6312.e22 (2021).
This paper reports structures of full-length mouse NLRP3 in oligomeric forms dubbed cages (dodecamer to hexadecamer) that hide the effector PYD inside, and implicates a role for cages in dispersion of the trans-Golgi network.
141. Ohto, U. et al. Structural basis for the oligomerization-mediated regulation of NLRP3 inflammasome activation. *Proc. Natl Acad. Sci. USA* **119**, e2121353119 (2022).
142. Misawa, T. et al. Microtubule-driven spatial arrangement of mitochondria promotes activation of the NLRP3 inflammasome. *Nat. Immunol.* **14**, 454–460 (2013).
143. Chen, J. & Chen, Z. J. PtdIns4P on dispersed trans-Golgi network mediates NLRP3 inflammasome activation. *Nature* **564**, 71–76 (2018).
144. Zhang, Z. et al. Distinct changes in endosomal composition promote NLRP3 inflammasome activation. *Nat. Immunol.* **24**, 30–41 (2023).
145. Li, X. et al. MARK4 regulates NLRP3 positioning and inflammasome activation through a microtubule-dependent mechanism. *Nat. Commun.* **8**, 15986 (2017).
146. Magupalli, V. G. et al. HDAC6 mediates an aggresome-like mechanism for NLRP3 and pyrin inflammasome activation. *Science* **369**, eaas8995 (2020).
147. Tapia-Abellan, A. et al. Sensing low intracellular potassium by NLRP3 results in a stable open structure that promotes inflammasome activation. *Sci. Adv.* **7**, eabf4468 (2021).
148. Bittner, Z. A. et al. BTK operates a phospho-tyrosine switch to regulate NLRP3 inflammasome activity. *J. Exp. Med.* **218**, e20201656 (2021).
149. Subramanian, N., Natarajan, K., Clatworthy, M. R., Wang, Z. & Germain, R. N. The adaptor MAVS promotes NLRP3 mitochondrial localization and inflammasome activation. *Cell* **153**, 348–361 (2013).
150. Park, S. et al. The mitochondrial antiviral protein MAVS associates with NLRP3 and regulates its inflammasome activity. *J. Immunol.* **191**, 4358–4366 (2013).
151. Gangopadhyay, A. et al. NLRP3 licenses NLRP11 for inflammasome activation in human macrophages. *Nat. Immunol.* **23**, 892–903 (2022).
152. He, M. et al. An acetylation switch of the NLRP3 inflammasome regulates aging-associated chronic inflammation and insulin resistance. *Cell Metab.* **31**, 580–591.e5 (2020).
153. Barry, R. et al. SUMO-mediated regulation of NLRP3 modulates inflammasome activity. *Nat. Commun.* **9**, 3001 (2018).
154. Song, H. et al. The E3 ubiquitin ligase TRIM31 attenuates NLRP3 inflammasome activation by promoting proteasomal degradation of NLRP3. *Nat. Commun.* **7**, 13727 (2016).
155. Chavarria-Smith, J., Mitchell, P. S., Ho, A. M., Daugherty, M. D. & Vance, R. E. Functional and evolutionary analyses identify proteolysis as a general mechanism for NLRP1 inflammasome activation. *PloS Pathog.* **12**, e1006052 (2016).
156. Zhong, F. L. et al. Germline NLRP1 mutations cause skin inflammatory and cancer susceptibility syndromes via inflammasome activation. *Cell* **167**, 187–202.e17 (2016).
157. Tschopp, J., Martinon, F. & Burns, K. NALPs: a novel protein family involved in inflammation. *Nat. Rev. Mol. Cell Biol.* **4**, 95–104 (2003).
158. Finger, J. N. et al. Autolytic proteolysis within the function to find domain (FIIND) is required for NLRP1 inflammasome activity. *J. Biol. Chem.* **287**, 25030–25037 (2012).
159. Chui, A. J. et al. N-Terminal degradation activates the NLRP1B inflammasome. *Science* **364**, 82–85 (2019).
160. Taabazuing, C. Y., Griswold, A. R. & Bachovchin, D. A. The NLRP1 and CARD8 inflammasomes. *Immunol. Rev.* **297**, 13–25 (2020).
161. Sandstrom, A. et al. Functional degradation: a mechanism of NLRP1 inflammasome activation by diverse pathogen enzymes. *Science* **364**, eaau1330 (2019).
162. D'Osualdo, A. et al. CARD8 and NLRP1 undergo autoproteolytic processing through a ZU5-like domain. *PloS ONE* **6**, e27396 (2011).
163. Mitchell, P. S., Sandstrom, A. & Vance, R. E. The NLRP1 inflammasome: new mechanistic insights and unresolved mysteries. *Curr. Opin. Immunol.* **60**, 37–45 (2019).
164. Levinsohn, J. L. et al. Anthrax lethal factor cleavage of Nlrp1 is required for activation of the inflammasome. *PloS Pathog.* **8**, e1002638 (2012).
165. Chavarria-Smith, J. & Vance, R. E. Direct proteolytic cleavage of NLRP1B is necessary and sufficient for inflammasome activation by anthrax lethal factor. *PloS Pathog.* **9**, e1003452 (2013).
166. Boyden, E. D. & Dietrich, W. F. Nalp1b controls mouse macrophage susceptibility to anthrax lethal toxin. *Nat. Genet.* **38**, 240–244 (2006).
167. Xu, H. et al. The N-end rule ubiquitin ligase UBR2 mediates NLRP1B inflammasome activation by anthrax lethal toxin. *EMBO J.* **38**, e101996 (2019).
168. Gai, K. et al. DPP8/9 inhibitors are universal activators of functional NLRP1 alleles. *Cell Death Dis.* **10**, 587 (2019).
169. Okondo, M. C. et al. Inhibition of Dpp8/9 activates the Nlrp1b inflammasome. *Cell Chem. Biol.* **25**, 262–267.e5 (2018).
170. Johnson, D. C. et al. DPP8/DPP9 inhibitor-induced pyroptosis for treatment of acute myeloid leukemia. *Nat. Med.* **24**, 1151–1156 (2018).

171. Zhong, F. L. et al. Human DPP9 represses NLRP1 inflammasome and protects against autoinflammatory diseases via both peptidase activity and FIIND domain binding. *J. Biol. Chem.* **293**, 18864–18878 (2018).
172. Sand, J. et al. Expression of inflammasome proteins and inflammasome activation occurs in human, but not in murine keratinocytes. *Cell Death Dis.* **9**, 24 (2018).
173. Fenini, G. et al. Genome editing of human primary keratinocytes by CRISPR/Cas9 reveals an essential role of the NLRP1 inflammasome in UVB sensing. *J. Investig. Dermatol.* **138**, 2644–2652 (2018).
174. Wu, C. C., Peterson, A., Zinshteyn, B., Regot, S. & Green, R. Ribosome collisions trigger general stress responses to regulate cell fate. *Cell* **182**, 404–416.e14 (2020).
175. Vind, A. C. et al. ZAKα recognizes stalled ribosomes through partially redundant sensor domains. *Mol. Cell* **78**, 700–713.e7 (2020).
176. Jenster, L. M. et al. P38 kinases mediate NLRP1 inflammasome activation after ribotoxic stress response and virus infection. *J. Exp. Med.* **220**, e20220837 (2023).
177. Robinson, K. S. et al. ZAKα-driven ribotoxic stress response activates the human NLRP1 inflammasome. *Science* **377**, 328–335 (2022).
178. Robinson, K. S. et al. Enteroviral 3C protease activates the human NLRP1 inflammasome in airway epithelia. *Science* **370**, eaay2002 (2020).
179. Tsu, B. V. et al. Diverse viral proteases activate the NLRP1 inflammasome. *eLife* **10**, e60609 (2021).
180. Bauernfried, S., Scherr, M. J., Pichlmair, A., Duderstadt, K. E. & Hornung, V. Human NLRP1 is a sensor for double-stranded RNA. *Science* **371**, eabd0811 (2021).
181. Ball, D. P. et al. Oxidized thioredoxin-1 restrains the NLRP1 inflammasome. *Sci. Immunol.* **7**, eabm7200 (2022).
182. Wang, Q. et al. The NLRP1 and CARD8 inflammasomes detect reductive stress. *Cell Rep.* **42**, 111966 (2023).
183. Orth-He, E. L. et al. Protein folding stress potentiates NLRP1 and CARD8 inflammasome activation. *Cell Rep.* **42**, 111965 (2023).
184. Huang, M. et al. Structural and biochemical mechanisms of NLRP1 inhibition by DPP9. *Nature* **592**, 773–777 (2021).
This paper reports the structure of an inhibitory ternary complex comprising rat NLRP1, its C-terminal domain and the dipeptidase DPP9.
185. Hollingsworth, L. R. et al. DPP9 sequesters the C terminus of NLRP1 to repress inflammasome activation. *Nature* **592**, 778–783 (2021).
This paper reports the structure of an inhibitory ternary complex comprising human NLRP1, its C-terminal domain and the dipeptidase DPP9.
186. Levandowski, C. B. et al. NLRP1 haplotypes associated with vitiligo and autoimmunity increase interleukin-1β processing via the NLRP1 inflammasome. *Proc. Natl Acad. Sci. USA* **110**, 2952–2956 (2013).
187. Jin, Y. et al. NALP1 in vitiligo-associated multiple autoimmune disease. *N. Engl. J. Med.* **356**, 1216–1225 (2007).
188. Grandemange, S. et al. A new autoinflammatory and autoimmune syndrome associated with NLRP1 mutations: NAIAD (NLRP1-associated autoinflammation with arthritis and dyskeratosis). *Ann. Rheum. Dis.* **76**, 1191–1198 (2017).
189. Ball, D. P. et al. Caspase-1 interdomain linker cleavage is required for pyroptosis. *Life Sci. Alliance* **3**, e202000664 (2020).
190. Jin, T., Curry, J., Smith, P., Jiang, J. & Xiao, T. S. Structure of the NLRP1 caspase recruitment domain suggests potential mechanisms for its association with procaspase-1. *Proteins* **81**, 1266–1270 (2013).
191. Bagnall, R. D. et al. Novel isoforms of the CARD8 (TUCAN) gene evade a nonsense mutation. *Eur. J. Hum. Genet.* **16**, 619–625 (2008).
192. Sharif, H. et al. Dipeptidyl peptidase 9 sets a threshold for CARD8 inflammasome formation by sequestering its active C-terminal fragment. *Immunity* **54**, 1392–1404.e10 (2021).
193. Wang, Q. et al. CARD8 is an inflammasome sensor for HIV-1 protease activity. *Science* **371**, eabe1707 (2021).
194. Tsu, B. V. et al. Host-specific sensing of coronaviruses and picornaviruses by the CARD8 inflammasome. *PloS Biol.* **21**, e3002144 (2023).
195. Nadkarni, R. et al. Viral proteases activate the CARD8 inflammasome in the human cardiovascular system. *J. Exp. Med.* **219**, e20212117 (2022).
196. Agard, N. J., Maltby, D. & Wells, J. A. Inflammatory stimuli regulate caspase substrate profiles. *Mol. Cell Proteom.* **9**, 880–893 (2010).
197. Sarhan, J. et al. Caspase-8 induces cleavage of gasdermin D to elicit pyroptosis during *Yersinia* infection. *Proc. Natl Acad. Sci. USA* **115**, E10888–E10897 (2018).
198. Orning, P. et al. Pathogen blockade of TAK1 triggers caspase-8-dependent cleavage of gasdermin D and cell death. *Science* **362**, 1064–1069 (2018).
199. Yu, P. et al. Pyroptosis: mechanisms and diseases. *Signal Transduct. Target. Ther.* **6**, 128 (2021).
200. Xia, X., Wang, X., Zheng, Y., Jiang, J. & Hu, J. What role does pyroptosis play in microbial infection? *J. Cell Physiol.* **234**, 7885–7892 (2019).
201. Shi, J., Gao, W. & Shao, F. Pyroptosis: gasdermin-mediated programmed necrotic cell death. *Trends Biochem. Sci.* **42**, 245–254 (2017).
202. Kayagaki, N. et al. NINJ1 mediates plasma membrane rupture during lytic cell death. *Nature* **591**, 131–136 (2021).
203. Liu, Z. et al. Crystal structures of the full-length murine and human gasdermin D reveal mechanisms of autoinhibition, lipid binding, and oligomerization. *Immunity* **51**, 43–49.e4 (2019).
204. Yang, J. et al. Mechanism of gasdermin D recognition by inflammatory caspases and their inhibition by a gasdermin D-derived peptide inhibitor. *Proc. Natl Acad. Sci. USA* **115**, 6792–6797 (2018).
205. Wang, K. et al. Structural mechanism for GSDMD targeting by autoprocessed caspases in pyroptosis. *Cell* **180**, 941–955.e20 (2020).
This paper reports the structures of caspase-4 and caspase-11, both in complex with GSDMD C-terminus, revealing the important exosite on the caspases for GSDMD recruitment.
206. Liu, Z. et al. Caspase-1 engages full-length gasdermin D through two distinct interfaces that mediate caspase recruitment and substrate cleavage. *Immunity* **53**, 106–114.e5 (2020).
This paper reports the structure of caspase-1 in complex with full-length GSDMD, revealing a two-site engagement, a caspase exosite interaction with GSDMD C-terminus and the caspase active site interaction with the N-terminal to C-terminal linker of GSDMD.
207. Ruan, J., Xia, S., Liu, X., Lieberman, J. & Wu, H. Cryo-EM structure of the gasdermin A3 membrane pore. *Nature* **557**, 62–67 (2018).
This paper reports the first gasdermin pore structure, revealing its β-barrel architecture, conformational change, lipid interaction and the existence of a prepore oligomer without membrane insertion.
208. Mulvihill, E. et al. Mechanism of membrane pore formation by human gasdermin-D. *EMBO J.* **37**, e98321 (2018).
209. Wang, C. et al. Structural basis for GSDMB pore formation and its targeting by IpaH7.8. *Nature* **616**, 590–597 (2023).
210. Zhong, X. et al. Structural mechanisms for regulation of GSDMB pore-forming activity. *Nature* **616**, 598–605 (2023).
211. Evavold, C. L. et al. The pore-forming protein gasdermin D regulates interleukin-1 secretion from living macrophages. *Immunity* **48**, 35–44.e6 (2018).
212. Xie, W. J., Xia, S., Warshel, A. & Wu, H. Electrostatic influence on IL-1 transport through the GSDMD pore. *Proc. Natl Acad. Sci. USA* **119**, e2120287119 (2022).
213. Keller, M., Ruegg, A., Werner, S. & Beer, H. D. Active caspase-1 is a regulator of unconventional protein secretion. *Cell* **132**, 818–831 (2008).
214. Chao, Y. Y. et al. Human T_H17 cells engage gasdermin E pores to release IL-1α on NLRP3 inflammasome activation. *Nat. Immunol.* **24**, 295–308 (2023).
215. Araki, T. & Milbrandt, J. Ninjurin2, a novel homophilic adhesion molecule, is expressed in mature sensory and enteric neurons and promotes neurite outgrowth. *J. Neurosci.* **20**, 187–195 (2000).
216. Araki, T. & Milbrandt, J. Ninjurin, a novel adhesion molecule, is induced by nerve injury and promotes axonal growth. *Neuron* **17**, 353–361 (1996).
217. Degen, M. et al. Structural basis of NINJ1-mediated plasma membrane rupture in cell death. *Nature* **618**, 1065–1071 (2023).
This paper reports the first structure of a NINJ1 oligomer in a double filament and proposes a NINJ1 filament and pore model for membrane damage.
218. Sahoo, B., Mou, Z., Liu, W., Dubyak, G. & Dai, X. How NINJ1 mediates plasma membrane rupture and why NINJ2 cannot. Preprint at *bioRxiv* https://doi.org/10.1101/2023.05.31.543175 (2023).
This preprint reports the structures of NINJ1 and NINJ2 oligomers in double filaments and proposes why NINJ1 oligomers, but not NINJ2 oligomers, are active for membrane rupture.
219. David, L. et al. NINJ1 mediates plasma membrane rupture through formation of nanodisc-like rings. Preprint at *bioRxiv* https://doi.org/10.1101/2023.06.01.543231 (2023).
This preprint reports the structure of a NINJ1 oligomer in a ring form with hydrophobic interior, which suggests a nanodisc model for membrane damage.

Acknowledgements

We apologize for incomplete citations owing to space limitations. The work was supported by the National Institutes of Health grants AI124491, AI139914 and AI177778 to H.W. and by the National Health and Medical Research Council of Australia grants 2009677 and 2009075 to K.S.

Author contributions

J.F. drafted the article, and all authors edited the article before submission.

Competing interests

H.W. is a co-founder and chair of the Scientific Advisory Board of Ventus Therapeutics. K.S. is a co-inventor on patent applications for NLRP3 inhibitors that have been licensed to Inflazome Ltd, which was acquired by Roche. K.S. served on the Scientific Advisory Board of Inflazome, Ireland, and Quench Bio, USA, and serves on a Scientific Advisory Board for Novartis, Switzerland. J.F. declares no competing interests.

Additional information

Peer review information *Nature Reviews Immunology* thanks Z. Hu and the other, anonymous, reviewer(s) for their contribution to the peer review of this work.